Hindawi
Advances in Mathematical Physics
Volume 2022, Article ID 7265164, 15 pages
https://doi.org/10.1155/2022/7265164

Research Article

Optical Wave Phenomena in Birefringent Fibers Described by Space-Time Fractional Cubic-Quartic Nonlinear Schrödinger Equation with the Sense of Beta and Conformable Derivative

M. F. Uddin and M. G. Hafez

Department of Mathematics, Chittagong University of Engineering and Technology, Chattogram 4349, Bangladesh

Correspondence should be addressed to M. F. Uddin; farhad.math@cuet.ac.bd and M. G. Hafez; hafez@cuet.ac.bd

Received 19 September 2022; Revised 30 November 2022; Accepted 1 December 2022; Published 16 December 2022

Academic Editor: Ivan Giorgio

The work explores the optical wave solutions along with their graphical representations by proposing the coupled spatial-temporal fractional cubic-quartic nonlinear Schrödinger equation with the sense of two fractal derivatives (beta and conformable derivative) and Kerr law nonlinearity for birefringent fibers. The new extended direct algebraic method for the first time is implemented to achieve this goal. Many optical solutions are listed along with their existence criteria. Based on the existence criteria, the cubic-quartic bright, and singular optical soliton, periodic pulse, and rouge wave profiles are supported in birefringent fibers with the influence of both beta and conformable derivative parameter.

1. Introduction

It is confirmed that the most idyllic information transferors, have the most captivating phenomena in fiber optics due to their expanding applications in optoelectronics, optical switching, optical metamaterials, telecommunications, and ultrafast signal processing systems [1–4]. As a result, one may study several nonlinear phenomena occurring on the aforementioned applications, namely nonlinear phase modulation, optical solitons, parametric and stimulated scattering processes, and supercontinuum generation. Such phenomena involving of different functions are very useful to understand the dynamical wave propagation in the area of all optical signal processing, namely optical amplification, multiwavelength sources, pulse generation, optical regeneration, wavelength conversion, and optical switching. The nonlinear Schrödinger equation (NLSE) is only the mathematical physics equation that characterizes the propagation of optical wave phenomena with different types of nonlinear media [5–9]. Over the past couple of decades, the majority of extant research has mostly focused on optical solitons in polarization-preserving fibers. However, solitons receive far less attention in birefringent fibers where the dynamics of soliton propagation are dictated by coupled NLSE [10–14]. As a result, the study of optical solitons in birefringent fibers is currently an important topic of nonlinear optics research.

Actually, the optical pulses traveling through an optical fiber tend to become polarized due to fiber nonuniformities, random changes in fiber diameter, and other technical issues caused by fiber technologies such as fiber twists, bends, and external stress. Such causes yield various problems, including differential group delay of the pulses, which is known as the polarization mode dispersion [15]. As a result, the dispersion has a significant negative impact on the steady and stable transmission of pulses across transcontinental and transoceanic lengths via fiber. At this stage, a phenomenon referred to as birefringence, which is caused by the splitting of optical pulses into two orthogonally polarized pulses. Thus, the birefringence is basically one kind of physical phenomenon in optical fibers with variable propagation constants and group velocities. It is also generated due to have delicate circular symmetry for optical fibers [16]. In such an undesirable physical state, the controlling NLSE in the birefringent fibers (BFs) breaks into vector coupled NLSE.

Furthermore, the notion of cubic-quartic (CQ) solitons is occurred due to the delicate balance between chromatic

dispersion (CD) and self-phase modulation becomes fragile with the CD becomes low enough. In order to restore the much-needed equilibrium in this crisis situation for the compensation of low CD count, the third-order dispersion (3OD) and fourth-order dispersion (4OD) terms are needed. This phenomenon is known as the CQ dispersive effects and it was firstly introduced in 2017 [17, 18]. Consequently, this study has been garnered a lot of interest in the research community from 2017 until the present. Recently, a group of researchers [19–22] have made a momentous effort to recover a slew of remarkable results for CQ optical solitons in Bragg-gratings fiber, magneto-optic wave–guides described by NLSEs and the newly proposed Biswas-Milovic equation. Besides, a few results have been reported on CQ solitons in birefringent fibres with different laws of refractive index using various efficient mathematical methodologies [23–27]. Therefore, it is imperative to focus on the previous studies along with their limitations as a follow-up. One of the significant flaws of previous studies are illustrated that they have solely considered the physical models for localization.

However, the fractional calculus has advanced over the last several decades. It is now well established that the influence of memory has been of major importance in the localization of modeling for quite some time. Profoundly, the integer-order physical models do not handle this memory issue efficiently [28, 29]. Many scholars have demonstrated that the noninteger operators can provide more information about the memory effect [30–32]. Consequently, the fractal derivatives, that is beta fractional derivative (BFD) and conformable fractional derivative (CFD) have been established recently as the extensions of integer order derivatives. Such derivatives play a dynamic role in modeling to study the local/nonlocal and conservative/nonconservative physical systems. The development of BFD and CFD meet many features of fundamental calculus, whereas the earlier fractional derivatives does not support some features of fundamental calculus. In References [33–38], authors have been used such derivatives for describing a wide range of physical processes. For instance, Uddin et al. [33–36] have reported that the effect of BFD parameter on nonlinear wave phenomena by considering different kinds of environments. Hafez et al. [37] and Iqbal et al. [38] have reported that the effect of CFD parameter on wave phenomena with their dynamical features in optical bullets and one-dimensional nonlinear electrical transmission line, respectively. It is now required to investigate nonlocal and nonconservative physical issues in optical fibers due to imperfections/nonuniformities in birefringent fibres along with some technical challenges resulting from fiber technologies discussed previously.

Thus, this work explores some new solutions with their better visualization on the topic of optical wave propagation in BFs described by the model of the governing coupled space-time fractional cubic-quartic NLSE (STF-CQNLSE) via the new extended direct algebraic method (EDAM) [39]. It is noted that the EDAM technique is first time implemented to achieve this goal for the considered model STF-CQNLSE along with the Kerr law of nonlinear refractive index in the presence of BFD and CFD. In addition, this work reveals mysteries of nonlocal behavior in birefringent fibers for the governing STF-CQNLSE by securing bright, singular, periodic singular, combo, and pure periodic optical soliton solutions with constraint criteria that must remain valid for these optical wave propagation to exist. The rest of this paper is organized as follows. The governing model equations are presented in the next subsections. Section 2 discusses the essential mathematical preliminaries for deriving the converted ordinary differential equation (ODE) from the leading STF-CQNLSE, which is described in Section 3. In Section 4, use the EDAM approach to recover the desired optical solitons. Section 5 discusses the graphical depiction of certain acquired results along with the comparison of previously reported outcomes. Finally, in Section 6, some closing observations are presented.

1.1. Governing Coupled Equation Having BFD and CFD Evolution. For polarization preserving fibers, the wave propagation through optical fibers with Kerr law of nonlinear refractive index is examined by the following cubic-quartic NLSE [23, 24].

$$i\phi_t + ip\phi_{xxx} + q\phi_{xxxx} + r|\phi|^2\phi = 0, \tag{1}$$

where the complex–valued function $\phi(x, t)$ is measuring the optical wave propagation in polarization preserving fibers, x (t) is the spatial (temporal) variable, r is the Kerr law of refractive index, respectively. The coefficients p and q are real constants represent the 3OD and 4OD, respectively. Note that most optical fibers are supported Kerr law nonlinearity. Recently, the fractional NLSEs (FNLSEs) are modeled and introduced to describe the physical process rather than NLSEs in the actual case especially in the field of nonlinear optical environments. To illustrate it, in References [40, 41], authors have reported the transmission dynamics of the beam describing by the FNLSE by considering fractional diffraction effect and self-defocusing saturable nonlinear media. They have studied the existence and dynamical evolution of fundamental solitons and multipole solitons supported by PT-symmetric potential. Wang and Wang [42] have studied the propagation of optical signal in fibers by considering the variable-coefficient wick-type stochastic FNLSE and found some analytical white noise functional solutions. They have shown that the FNLSEs can support a variety of new fractional optical solitons, such as multipole solitons, chirped and chirp-free fractional bright and dark soliton, and symmetric and antisymmetric solitons. Uddin et al. [33] have reported that one can derive nonlinear evolution equations of fractional order from nonlinear evolution equations of integer order using Agrawal's variational principle when the complexity arises in a certain regimes of space or time for the impact of nonlocality as well as nonconservative energies arising in the physical systems. For the sake of simplicity, instead of deriving the fractional order equation, the following coupled STF-CQNLSE which incorporates BFD into consideration for the nonlocal nonlinear media and draws inspiration from the aforementioned literatures, is presented in this study to characterize the nonlocal behavior in BFs when the pulses are split into two direction frames from Equation (1):

$$i\left({}_0^A\mathscr{D}_t^{\mu}\Psi_1\right)+ip_1\left({}_0^A\mathscr{D}_x^{3\mu}\Psi_1\right)+q_1\left({}_0^A\mathscr{D}_x^{4\mu}\Psi_1\right)+\left(r_1\left|\Psi_1^2\right|+s_1\left|\Psi_2^2\right|\right)\Psi_1=0,$$
$$i\left({}_0^A\mathscr{D}_t^{\mu}\Psi_2\right)+ip_2\left({}_0^A\mathscr{D}_x^{3\mu}\Psi_2\right)+q_2\left({}_0^A\mathscr{D}_x^{4\mu}\Psi_2\right)+\left(r_2\left|\Psi_2^2\right|+s_2\left|\Psi_1^2\right|\right)\Psi_2=0. \tag{2}$$

Whereas the STF-CQNLSE is described in terms of CFD by

$$i\mathscr{D}_t^{\mu}\Psi_1+ip_1\mathscr{D}_x^{3\mu}\Psi_1+q_1\mathscr{D}_x^{4\mu}\Psi_1+\left(r_1\left|\Psi_1^2\right|+s_1\left|\Psi_2^2\right|\right)\Psi_1=0,$$
$$i\mathscr{D}_t^{\mu}\Psi_2+ip_2\mathscr{D}_x^{3\mu}\Psi_2+q_2\mathscr{D}_x^{4\mu}\Psi_2+\left(r_2\left|\Psi_2^2\right|+s_2\left|\Psi_1^2\right|\right)\Psi_2=0. \tag{3}$$

In the above coupled systems, r_j (s_j), $j=1,2$ indicated the coefficients of self-phase modulation (cross-phase modulation)and the effect of four–wave mixing is discarded. Many researchers [40–47] have already implemented several kinds of mathematical procedures to solve the evolution equations involving of local and nonlocal operators. The solutions of Equations (2) and (3) have already been determined in the earlier investigations [23, 24] via the Riccati function, Sine-Gordon function, F–expansion, and exp-function expansion methods by considering only the classical models i.e. when $\mu=1$. However, EDAM will be implemented to determine the traveling wave solutions of Equations (2) and (3) with the presence of nonlocal operators.

2. Mathematical Preliminaries

2.1. Beta Fractional Derivative (BFD). The useful definition of BFD is recently introduced by the scholar group Atangana et al. [48].

Definition 1. Let $a\in\mathfrak{R}$ and $\mathscr{G}$ be a function such that $\mathscr{G}:[a,\infty)\longrightarrow\mathfrak{R}$. Then the beta fractional derivative of order μ of $\mathscr{G}$ is exhibited as ${}_0^A\mathscr{D}_x^{\mu}\mathscr{G}(x)$ and defined by

$${}_0^A\mathscr{D}_x^{\mu}\mathscr{G}(x)=\lim_{\varsigma\longrightarrow 0}\frac{\mathscr{G}\left(x+\varsigma(x+(1/\Gamma(\mu)))^{1-\mu}\right)-\mathscr{G}(x)}{\varsigma};\quad 0<\mu\le 1. \tag{4}$$

Properties 2. Let $0<\mu\le 1$ and suppose that $\alpha,\alpha_1,\alpha_2\in\mathfrak{R}$, $\mathscr{F}$, $\mathscr{G}\neq 0$ are two beta-differentiable functions of order μ. Then

$$\begin{aligned}
{}_0^A\mathscr{D}_x^{\mu}\{\alpha_1\mathscr{F}(x)+\alpha_2\mathscr{G}(x)\}&=\alpha_1{}_0^A\mathscr{D}_x^{\mu}\{\mathscr{F}(x)\}+\alpha_2{}_0^A\mathscr{D}_x^{\mu}\{\mathscr{G}(x)\},\\
{}_0^A\mathscr{D}_x^{\mu}\{\alpha\}&=0,\\
{}_0^A\mathscr{D}_x^{\mu}\{\mathscr{F}(x)\cdot\mathscr{G}(x)\}&=\mathscr{F}(x)\cdot{}_0^A\mathscr{D}_x^{\mu}\{\mathscr{G}(x)\}+\mathscr{G}(x)\cdot{}_0^A\mathscr{D}_x^{\mu}\{\mathscr{F}(x)\},\\
{}_0^A\mathscr{D}_x^{\mu}\{\mathscr{F}(x)/\mathscr{G}(x)\}&=\frac{\mathscr{G}(x)\cdot{}_0^A\mathscr{D}_x^{\mu}\{\mathscr{F}(x)\}-\mathscr{F}(x)\cdot{}_0^A\mathscr{D}_x^{\mu}\{\mathscr{G}(x)\}}{\mathscr{G}^2(x)}.
\end{aligned} \tag{5}$$

It is noted that if one introduce $\varsigma=(x+(1/\Gamma(\mu)))^{\mu-1}\mathfrak{h}$, when $\varsigma\longrightarrow 0$, $\mathfrak{h}\longrightarrow 0$ in Equation (4), one of the most important property of BFD is defined as

$${}_0^A\mathscr{D}_x^{\mu}\mathscr{G}(x)=\left(x+\frac{1}{\Gamma(\mu)}\right)^{1-\mu}\frac{d\mathscr{G}(x)}{dx}. \tag{6}$$

which is indicated that the BFD can not only be treated as fractional derivative but also as a natural extension of the integer order derivative.

2.2. Conformable Fractional Derivative (CFD). Khalil et al. [49] are introduced in details about the CFD with the following useful definition.

Definition 3. Assume that $\mathscr{G}$ be a function such that $\mathscr{G}:[0,\infty)\longrightarrow\mathfrak{R}$. Then the conformable fractional derivative of order μ of $\mathscr{G}$ is denoted as $\mathscr{D}_x^{\mu}\mathscr{G}(x)$ and given by

$$\mathscr{D}_x^{\mu}\mathscr{G}(x)=\lim_{\varsigma\longrightarrow 0}\frac{\mathscr{G}\left(x+\varsigma x^{1-\mu}\right)-\mathscr{G}(x)}{\varsigma};\quad 0<\mu\le 1. \tag{7}$$

Properties 4. Suppose that $0<\mu\le 1$ and assuming $\alpha,a,b,c\in\mathfrak{R}$, $\mathscr{F},\mathscr{G}\neq 0$ are two functions conformable differentiable of order μ. Then

$$\begin{aligned}
\mathscr{D}_x^{\mu}(x^{\alpha})&=\alpha x^{\alpha-\mu},\\
\mathscr{D}_x^{\mu}(c)&=0,\\
\mathscr{D}_x^{\mu}\{a\mathscr{F}(x)+b\mathscr{G}(x)\}&=a\mathscr{D}_x^{\mu}\{\mathscr{F}(x)\}+b\mathscr{D}_x^{\mu}\{\mathscr{G}(x)\},\\
\mathscr{D}_x^{\mu}\{\mathscr{F}(x)\cdot\mathscr{G}(x)\}&=\mathscr{F}(x)\cdot\mathscr{D}_x^{\mu}\{\mathscr{G}(x)\}+\mathscr{G}(x)\cdot\mathscr{D}_x^{\mu}\{\mathscr{F}(x)\},\\
\mathscr{D}_x^{\mu}\{\mathscr{F}(x)/\mathscr{G}(x)\}&=\frac{\mathscr{G}(x)\cdot\mathscr{D}_x^{\mu}\{\mathscr{F}(x)\}-\mathscr{F}(x)\cdot\mathscr{D}_x^{\mu}\{\mathscr{G}(x)\}}{\mathscr{G}^2(x)},\\
\mathscr{D}_x^{\mu}\{\mathscr{G}(x)\}&=x^{1-\mu}\frac{d\mathscr{G}(x)}{dx}.
\end{aligned} \tag{8}$$

3. Converted ODE for STF-CQNLSE

To start with the following traveling wave variables transform to convert the systems of Equations(2) and (3) into its corresponding ODEs:

$$\begin{aligned}
\Psi_1(x,t)&=\mathscr{E}_1\left(\Xi_j\right)e^{i\mathfrak{T}_j(x,t)},\\
\Psi_2(x,t)&=\mathscr{E}_2\left(\Xi_j\right)e^{i\mathfrak{T}_j(x,t)}.
\end{aligned} \tag{9}$$

where $j=\{\mathscr{B},\mathscr{C}\}$. The real functions $\mathscr{E}_i(\Xi_j)$ and $\mathfrak{T}_j(x,t)$ are representing the amplitude portion and the phase component of the pulse wave propagation, respectively. It is noted here that $\Xi_{\mathscr{B}}$ and $\mathfrak{T}_{\mathscr{B}}$ are considered for BFD and defined by

$$\begin{aligned}
\Xi_{\mathscr{B}}&=\frac{1}{\mu}\left(x+\frac{1}{\Gamma\mu}\right)^{\mu}-\frac{\nu}{\mu}\left(t+\frac{1}{\Gamma\mu}\right)^{\mu},\\
\mathfrak{T}_{\mathscr{B}}&=-\frac{\kappa}{\mu}\left(x+\frac{1}{\Gamma\mu}\right)^{\mu}+\frac{\omega}{\mu}\left(t+\frac{1}{\Gamma\mu}\right)^{\mu}+\theta_0.
\end{aligned} \tag{10}$$

whereas in sense of CFD, $\Xi_{\mathscr{C}}$, and $\mathfrak{T}_{\mathscr{C}}$ are defined by

$$\begin{aligned}\Xi_{\mathscr{C}} &= \frac{1}{\mu}x^{\mu} - \frac{\nu}{\mu}t^{\mu},\\ \mathfrak{T}_{\mathscr{C}} &= -\frac{\kappa}{\mu}x^{\mu} + \frac{\omega}{\mu}t^{\mu} + \theta_0.\end{aligned} \tag{11}$$

Here ν, κ, ω, and θ_0 are representing the speed, frequency, number, and phase constant of wave, respectively. The coupled system of Equation (2) and Equation (3) are then converted to the same ODEs by substituting separately the pair of equations, either Equation (9) and Equation (10) for BFD or Equation (9) and Equation (11) for CFD along with their suitable properties. Finally, for the sake of simplicity of this report, after decomposing the obtained ODEs into real and imaginary parts, one attains the following:

Real parts:

$$\begin{aligned}&q_1\mathscr{E}_1^{(iv)} + \left(3\kappa p_1 - 6\kappa^2 q_1\right)\mathscr{E}_1'' + \left(\kappa^4 q_1 - \kappa^3 p_1 - \omega\right)\mathscr{E}_1 + r_1\mathscr{E}_1^3 + s_1\mathscr{E}_1\mathscr{E}_2^2 = 0,\\ &q_2\mathscr{E}_2^{(iv)} + \left(3\kappa p_2 - 6\kappa^2 q_2\right)\mathscr{E}_2'' + \left(\kappa^4 q_2 - \kappa^3 p_2 - \omega\right)\mathscr{E}_2 + r_2\mathscr{E}_2^3 + s_2\mathscr{E}_1^2\mathscr{E}_2 = 0,\end{aligned} \tag{12}$$

where the superscripts $\mathscr{E}_1^{(iv)}$, $\mathscr{E}_1'''$, $\mathscr{E}_1''$, and $\mathscr{E}_1'$ are denoted the fourth, third, second, and first order derivatives of $\mathscr{E}_1$, respectively.

Imaginary parts:

$$\begin{aligned}&\left(p_1 - 4\kappa q_1\right)\mathscr{E}_1''' - \left(\nu + 3\kappa^2 p_1 - 4\kappa^3 q_1\right)\mathscr{E}_1' = 0,\\ &\left(p_2 - 4\kappa q_2\right)\mathscr{E}_2''' - \left(\nu + 3\kappa^2 p_2 - 4\kappa^3 q_2\right)\mathscr{E}_2' = 0.\end{aligned} \tag{13}$$

Applying the linearly independent principle to imaginary parts for recovering:

$$\begin{aligned}\nu &= 4\kappa^3 q_1 - 3\kappa^2 p_1,\\ p_1 - 4\kappa q_1 &= 0.\\ \nu &= 4\kappa^3 q_2 - 3\kappa^2 p_2,\\ p_2 - 4\kappa q_2 &= 0.\end{aligned} \tag{14}$$

This two equations gives the frequency of waves as

$$\kappa = \frac{3(p_1 - p_2)}{4(q_1 - q_2)}. \tag{15}$$

This suggests that $p_1 \neq p_2$ and $q_1 \neq q_2$.

Setting $\mathscr{E}_2 = \Pi\mathscr{E}_1$, where Π is any nonzero constant so that $\Pi \neq 1$. The real parts implies to the following:

$$q_1\mathscr{E}_1^{(iv)} + \left(3\kappa p_1 - 6\kappa^2 q_1\right)\mathscr{E}_1'' + \left(\kappa^4 q_1 - \kappa^3 p_1 - \omega\right)\mathscr{E}_1 + \left(r_1 + \Pi^2 s_1\right)\mathscr{E}_1^3 = 0, \tag{16}$$

$$\Pi q_2\mathscr{E}_1^{(iv)} + \Pi\left(3\kappa p_2 - 6\kappa^2 q_2\right)\mathscr{E}_1'' + \Pi\left(\kappa^4 q_2 - \kappa^3 p_2 - \omega\right)\mathscr{E}_1 + \left(\Pi^3 r_2 + \Pi s_2\right)\mathscr{E}_1^3 = 0. \tag{17}$$

Both these equations have the similar form under the following constraint conditions:

$$\begin{aligned}q_1 &= \Pi q_2,\\ 3\kappa p_1 - 6\kappa^2 q_1 &= \Pi\left(3\kappa p_2 - 6\kappa^2 q_2\right),\\ \kappa^4 q_1 - \kappa^3 p_1 - \omega &= \Pi\left(\kappa^4 q_2 - \kappa^3 p_2 - \omega\right),\\ r_1 + \Pi^2 s_1 &= \Pi\left(\Pi^2 r_2 + s_2\right).\end{aligned} \tag{18}$$

Now, considering

$$Y_0 = 3\kappa p_1 - 6\kappa^2 q_1,\ Y_1 = \kappa^4 q_1 - \kappa^3 p_1,\ Y_2 = r_1 + \Pi^2 s_1, \tag{19}$$

Equation (16) reduces to the following form

$$q_1\mathscr{E}_1^{(iv)} + Y_0\mathscr{E}_1'' + (Y_1 - \omega)\mathscr{E}_1 + Y_2\mathscr{E}_1^3 = 0. \tag{20}$$

4. Analytical Solutions of STF-CQNLSE via EDAM

Applying the homogeneous balance principle to $\mathscr{E}_1^{(iv)}$ and $\mathscr{E}_1^3$ in Equation (20) and according to EDAM (see details in Reference [39]), the formal analytical solutions of Equation (20) can be represented as a polynomial in $\mathscr{S}(\Xi_j)$:

$$\mathscr{E}_1\left(\Xi_j\right) = \eta_0 + \sum_{L=1}^{2}\eta_L\mathscr{S}^L\left(\Xi_j\right), \tag{21}$$

where $\eta_L (L = 0, 1, 2)$ are constants with $\eta_2 \neq 0$. $\mathscr{S}(\Xi_j)$ is satisfied the following ODE:

$$\frac{d\mathscr{S}\left(\Xi_j\right)}{d\,\Xi_j} = \ln(\mathscr{A})\left(\alpha + \lambda\mathscr{S}\left(\Xi_j\right) + \sigma\mathscr{S}^2\left(\Xi_j\right)\right);\quad \mathscr{A} \neq 0, 1. \tag{22}$$

Note that Equation (22) offers a hung amount of solutions by depending on α, λ, and σ as set out in Reference [39]. By considering Equation (21) and Equation (22), a polynomial in $\mathscr{S}(\Xi_j)$ is obtained from Equation (20). As a result, a set of algebraic equations (ignored for convenience) for $\eta_0, \eta_1, \eta_2, \alpha, \lambda, \sigma$, and ω are formulated by setting the coefficients of this polynomial equal to zero. By simplifying such equations via the computational package Maple-18, the following relations are determined:

$$\begin{aligned}&\eta_0 = \pm 6\alpha\sigma(\ln(\mathscr{A}))^2\sqrt{-\frac{10\kappa p_1}{Y_2\mathscr{H}_1}}, \eta_1 = \pm 6\lambda\sigma(\ln(\mathscr{A}))^2\sqrt{-\frac{10\kappa p_1}{Y_2\mathscr{H}_1}},\\ &\eta_2 = \pm 6\sigma^2(\ln(\mathscr{A}))^2\sqrt{-\frac{10\kappa p_1}{Y_2\mathscr{H}_1}}, \omega = \frac{\mathscr{H}_1 Y_1 - 12(\ln(\mathscr{A}))^4\Phi^2\kappa p_1}{\mathscr{H}_1}, q_1 = \frac{3\kappa p_1}{\mathscr{H}_1}.\end{aligned} \tag{23}$$

where $\mathscr{H}_1 = 20\alpha\sigma(\ln(\mathscr{A}))^2 - 5\lambda^2(\ln(\mathscr{A}))^2 + 6\kappa^2$ and $\Phi = \lambda^2 - 4\alpha\sigma$.

By considering the above relations together with the solutions of Equation (22) and the assistance of Equation

(21), the following solitary wave solutions for the considered STF-CQNLSE as in Equation (2) and Equation (3) in sense of BFD and CFD, respectively, are determined:

Case 1. When $\Phi < 0$ and $\sigma \neq 0$,

$$\Psi_1^1(x,t) = \mp\frac{3\Phi}{2}(\ln(\mathscr{A}))^2\sqrt{-\frac{10\kappa p_1}{Y_2\mathscr{H}_1}}\left\{1+\tan_{\mathscr{A}}\left(\frac{\sqrt{-\Phi}}{2}\Xi_j\right)^2\right\}e^{i\mathfrak{T}_j}, \quad (24)$$

$$\Psi_2^1(x,t) = \mp\frac{3\Pi\Phi}{2}(\ln(\mathscr{A}))^2\sqrt{-\frac{10\kappa p_1}{Y_2\mathscr{H}_1}}\left\{1+\tan_{\mathscr{A}}\left(\frac{\sqrt{-\Phi}}{2}\Xi_j\right)^2\right\}e^{i\mathfrak{T}_j}, \quad (25)$$

$$\Psi_1^2(x,t) = \mp\frac{3\Phi}{2}(\ln(\mathscr{A}))^2\sqrt{-\frac{10\kappa p_1}{Y_2\mathscr{H}_1}}\left\{1+\cot_{\mathscr{A}}\left(\frac{\sqrt{-\Phi}}{2}\Xi_j\right)^2\right\}e^{i\mathfrak{T}_j}, \quad (26)$$

$$\Psi_2^2(x,t) = \mp\frac{3\Pi\Phi}{2}(\ln(\mathscr{A}))^2\sqrt{-\frac{10\kappa p_1}{Y_2\mathscr{H}_1}}\left\{1+\cot_{\mathscr{A}}\left(\frac{\sqrt{-\Phi}}{2}\Xi_j\right)^2\right\}e^{i\mathfrak{T}_j}, \quad (27)$$

$$\Psi_1^3(x,t) = \mp\frac{3\Phi}{2}(\ln(\mathscr{A}))^2\sqrt{-\frac{10\kappa p_1}{Y_2\mathscr{H}_1}}\left\{1+\left[\tan_{\mathscr{A}}\left(\sqrt{-\Phi}\Xi_j\right)\pm\sqrt{\mathscr{M}\mathscr{N}}\sec_{\mathscr{A}}\left(\sqrt{-\Phi}\Xi_j\right)\right]^2\right\}e^{i\mathfrak{T}_j}, \quad (28)$$

$$\Psi_2^3(x,t) = \mp\frac{3\Pi\Phi}{2}(\ln(\mathscr{A}))^2\sqrt{-\frac{10\kappa p_1}{Y_2\mathscr{H}_1}}\left\{1+\left[\tan_{\mathscr{A}}\left(\sqrt{-\Phi}\Xi_j\right)\pm\sqrt{\mathscr{M}\mathscr{N}}\sec_{\mathscr{A}}\left(\sqrt{-\Phi}\Xi_j\right)\right]^2\right\}e^{i\mathfrak{T}_j}, \quad (29)$$

$$\Psi_1^4(x,t) = \mp\frac{3\Phi}{2}(\ln(\mathscr{A}))^2\sqrt{-\frac{10\kappa p_1}{Y_2\mathscr{H}_1}}\left\{1+\left[\cot_{\mathscr{A}}\left(\sqrt{-\Phi}\Xi_j\right)\pm\sqrt{\mathscr{M}\mathscr{N}}\csc_{\mathscr{A}}\left(\sqrt{-\Phi}\Xi_j\right)\right]^2\right\}e^{i\mathfrak{T}_j}, \quad (30)$$

$$\Psi_2^4(x,t) = \mp\frac{3\Pi\Phi}{2}(\ln(\mathscr{A}))^2\sqrt{-\frac{10\kappa p_1}{Y_2\mathscr{H}_1}}\left\{1+\left[\cot_{\mathscr{A}}\left(\sqrt{-\Phi}\Xi_j\right)\pm\sqrt{\mathscr{M}\mathscr{N}}\csc_{\mathscr{A}}\left(\sqrt{-\Phi}\Xi_j\right)\right]^2\right\}e^{i\mathfrak{T}_j}, \quad (31)$$

$$\Psi_1^5(x,t) = \mp\frac{3\Phi}{8}(\ln(\mathscr{A}))^2\sqrt{-\frac{10\kappa p_1}{Y_2\mathscr{H}_1}}\left\{4+\left[\tan_{\mathscr{A}}\left(\frac{\sqrt{-\Phi}}{4}\Xi_j\right)-\cot_{\mathscr{A}}\left(\frac{\sqrt{-\Phi}}{4}\Xi_j\right)\right]^2\right\}e^{i\mathfrak{T}_j}, \quad (32)$$

$$\Psi_2^5(x,t) = \mp\frac{3\Pi\Phi}{8}(\ln(\mathscr{A}))^2\sqrt{-\frac{10\kappa p_1}{Y_2\mathscr{H}_1}}\left\{4+\left[\tan_{\mathscr{A}}\left(\frac{\sqrt{-\Phi}}{4}\Xi_j\right)-\cot_{\mathscr{A}}\left(\frac{\sqrt{-\Phi}}{4}\Xi_j\right)\right]^2\right\}e^{i\mathfrak{T}_j}. \quad (33)$$

Case 2. When $\Phi > 0$ and $\sigma \neq 0$,

$$\Psi_1^6(x,t) = \mp\frac{3\Phi}{2}(\ln(\mathscr{A}))^2\sqrt{-\frac{10\kappa p_1}{Y_2\mathscr{H}_1}}\left\{1-\tanh_{\mathscr{A}}\left(\frac{\sqrt{\Phi}}{2}\Xi_j\right)^2\right\}e^{i\mathfrak{T}_j}, \quad (34)$$

$$\Psi_2^6(x,t) = \mp\frac{3\Pi\Phi}{2}(\ln(\mathscr{A}))^2\sqrt{-\frac{10\kappa p_1}{Y_2\mathscr{H}_1}}\left\{1-\tanh_{\mathscr{A}}\left(\frac{\sqrt{\Phi}}{2}\Xi_j\right)^2\right\}e^{i\mathfrak{T}_j}, \quad (35)$$

$$\Psi_1^7(x,t) = \mp\frac{3\Phi}{2}(\ln(\mathscr{A}))^2\sqrt{-\frac{10\kappa p_1}{Y_2\mathscr{H}_1}}\left\{1-\coth_{\mathscr{A}}\left(\frac{\sqrt{\Phi}}{2}\Xi_j\right)^2\right\}e^{i\mathfrak{T}_j}, \quad (36)$$

$$\Psi_2^7(x,t) = \mp\frac{3\Pi\Phi}{2}(\ln(\mathscr{A}))^2\sqrt{-\frac{10\kappa p_1}{Y_2\mathscr{H}_1}}\left\{1-\coth_{\mathscr{A}}\left(\frac{\sqrt{\Phi}}{2}\Xi_j\right)^2\right\}e^{i\mathfrak{T}_j}, \quad (37)$$

$$\Psi_1^8(x,t) = \mp\frac{3\Phi}{2}(\ln(\mathscr{A}))^2\sqrt{-\frac{10\kappa p_1}{Y_2\mathscr{H}_1}}\left\{1-\left[\tanh_{\mathscr{A}}\left(\sqrt{\Phi}\Xi_j\right)\mp i\sqrt{\mathscr{M}\mathscr{N}}\sec h_{\mathscr{A}}\left(\sqrt{\Phi}\Xi_j\right)\right]^2\right\}e^{i\mathfrak{T}_j}, \quad (38)$$

$$\Psi_2^8(x,t) = \mp\frac{3\Pi\Phi}{2}(\ln(\mathscr{A}))^2\sqrt{-\frac{10\kappa p_1}{Y_2\mathscr{H}_1}}\left\{1-\left[\tanh_{\mathscr{A}}\left(\sqrt{\Phi}\Xi_j\right)\mp i\sqrt{\mathscr{M}\mathscr{N}}\sec h_{\mathscr{A}}\left(\sqrt{\Phi}\Xi_j\right)\right]^2\right\}e^{i\mathfrak{T}_j}, \quad (39)$$

$$\Psi_1^9(x,t) = \mp\frac{3\Phi}{2}(\ln(\mathscr{A}))^2\sqrt{-\frac{10\kappa p_1}{Y_2\mathscr{H}_1}}\left\{1-\left[\coth_{\mathscr{A}}\left(\sqrt{\Phi}\Xi_j\right)\mp\sqrt{\mathscr{M}\mathscr{N}}\csc h_{\mathscr{A}}\left(\sqrt{\Phi}\Xi_j\right)\right]^2\right\}e^{i\mathfrak{T}_j}, \quad (40)$$

$$\Psi_2^9(x,t) = \mp\frac{3\Pi\Phi}{2}(\ln(\mathscr{A}))^2\sqrt{-\frac{10\kappa p_1}{Y_2\mathscr{H}_1}}\left\{1-\left[\coth_{\mathscr{A}}\left(\sqrt{\Phi}\Xi_j\right)\mp\sqrt{\mathscr{M}\mathscr{N}}\csc h_{\mathscr{A}}\left(\sqrt{\Phi}\Xi_j\right)\right]^2\right\}e^{i\mathfrak{T}_j}, \quad (41)$$

$$\Psi_1^{10}(x,t) = \mp\frac{3\Phi}{8}(\ln(\mathscr{A}))^2\sqrt{-\frac{10\kappa p_1}{Y_2\mathscr{H}_1}}\left\{4-\left[\tanh_{\mathscr{A}}\left(\frac{\sqrt{\Phi}}{4}\Xi_j\right)+\coth_{\mathscr{A}}\left(\frac{\sqrt{\Phi}}{4}\Xi_j\right)\right]^2\right\}e^{i\mathfrak{T}_j}, \quad (42)$$

$$\Psi_2^{10}(x,t) = \mp\frac{3\Pi\Phi}{8}(\ln(\mathscr{A}))^2\sqrt{-\frac{10\kappa p_1}{Y_2\mathscr{H}_1}}\left\{4-\left[\tanh_{\mathscr{A}}\left(\frac{\sqrt{\Phi}}{4}\Xi_j\right)+\coth_{\mathscr{A}}\left(\frac{\sqrt{\Phi}}{4}\Xi_j\right)\right]^2\right\}e^{i\mathfrak{T}_j}. \quad (43)$$

Case 3. When $\alpha\sigma > 0$ and $\lambda = 0$,

$$\Psi_1^{11}(x,t) = \pm 6\alpha\sigma(\ln(\mathscr{A}))^2\sqrt{-\frac{10\kappa p_1}{Y_2\mathscr{H}_1}}\left\{1+\tan_{\mathscr{A}}\left(\sqrt{\alpha\sigma}\Xi_j\right)^2\right\}e^{i\mathfrak{T}_j},$$

$$\Psi_2^{11}(x,t) = \pm 6\Pi\alpha\sigma(\ln(\mathscr{A}))^2\sqrt{-\frac{10\kappa p_1}{Y_2\mathscr{H}_1}}\left\{1+\tan_{\mathscr{A}}\left(\sqrt{\alpha\sigma}\Xi_j\right)^2\right\}e^{i\mathfrak{T}_j},$$

$$\Psi_1^{12}(x,t) = \pm 6\alpha\sigma(\ln(\mathscr{A}))^2\sqrt{-\frac{10\kappa p_1}{Y_2\mathscr{H}_1}}\left\{1+\cot_{\mathscr{A}}\left(\sqrt{\alpha\sigma}\Xi_j\right)^2\right\}e^{i\mathfrak{T}_j},$$

$$\Psi_2^{12}(x,t) = \pm 6\Pi\alpha\sigma(\ln(\mathscr{A}))^2\sqrt{-\frac{10\kappa p_1}{Y_2\mathscr{H}_1}}\left\{1+\cot_{\mathscr{A}}\left(\sqrt{\alpha\sigma}\Xi_j\right)^2\right\}e^{i\mathfrak{T}_j},$$

$$\Psi_1^{13}(x,t) = \pm 6\alpha\sigma(\ln(\mathscr{A}))^2\sqrt{-\frac{10\kappa p_1}{Y_2\mathscr{H}_1}}\left\{1+\left[\tan_{\mathscr{A}}\left(2\sqrt{\alpha\sigma}\Xi_j\right)\pm\sqrt{\mathscr{M}\mathscr{N}}\sec_{\mathscr{A}}\left(2\sqrt{\alpha\sigma}\Xi_j\right)\right]^2\right\}e^{i\mathfrak{T}_j},$$

$$\Psi_2^{13}(x,t) = \pm 6\Pi\alpha\sigma(\ln(\mathscr{A}))^2\sqrt{-\frac{10\kappa p_1}{Y_2\mathscr{H}_1}}\left\{1+\left[\tan_{\mathscr{A}}\left(2\sqrt{\alpha\sigma}\Xi_j\right)\pm\sqrt{\mathscr{M}\mathscr{N}}\sec_{\mathscr{A}}\left(2\sqrt{\alpha\sigma}\Xi_j\right)\right]^2\right\}e^{i\mathfrak{T}_j},$$

$$\Psi_1^{14}(x,t) = \pm 6\alpha\sigma(\ln(\mathscr{A}))^2\sqrt{-\frac{10\kappa p_1}{Y_2\mathscr{H}_1}}\left\{1+\left[\cot_{\mathscr{A}}\left(2\sqrt{\alpha\sigma}\Xi_j\right)\mp\sqrt{\mathscr{M}\mathscr{N}}\csc_{\mathscr{A}}\left(2\sqrt{\alpha\sigma}\Xi_j\right)\right]^2\right\}e^{i\mathfrak{T}_j},$$

$$\Psi_2^{14}(x,t) = \pm 6\Pi\alpha\sigma(\ln(\mathscr{A}))^2\sqrt{-\frac{10\kappa p_1}{Y_2\mathscr{H}_1}}\left\{1+\left[\cot_{\mathscr{A}}\left(2\sqrt{\alpha\sigma}\Xi_j\right)\mp\sqrt{\mathscr{M}\mathscr{N}}\csc_{\mathscr{A}}\left(2\sqrt{\alpha\sigma}\Xi_j\right)\right]^2\right\}e^{i\mathfrak{T}_j},$$

$$\Psi_1^{15}(x,t) = \pm\frac{3}{2}\alpha\sigma(\ln(\mathscr{A}))^2\sqrt{-\frac{10\kappa p_1}{Y_2\mathscr{H}_1}}\left\{4+\left[\tan_{\mathscr{A}}\left(\frac{\sqrt{\alpha\sigma}}{2}\Xi_j\right)-\cot_{\mathscr{A}}\left(\frac{\sqrt{\alpha\sigma}}{2}\Xi_j\right)\right]^2\right\}e^{i\mathfrak{T}_j},$$

$$\Psi_2^{15}(x,t) = \pm\frac{3\Pi}{2}\alpha\sigma(\ln(\mathscr{A}))^2\sqrt{-\frac{10\kappa p_1}{Y_2\mathscr{H}_1}}\left\{4+\left[\tan_{\mathscr{A}}\left(\frac{\sqrt{\alpha\sigma}}{2}\Xi_j\right)-\cot_{\mathscr{A}}\left(\frac{\sqrt{\alpha\sigma}}{2}\Xi_j\right)\right]^2\right\}e^{i\mathfrak{T}_j}. \quad (44)$$

Case 4. When $\alpha\sigma < 0$ and $\lambda = 0$,

$$\Psi_1^{16}(x,t) = \pm 6\alpha\sigma(\ln(\mathscr{A}))^2\sqrt{-\frac{10\kappa p_1}{Y_2\mathscr{H}_1}}\left\{1-\tanh_{\mathscr{A}}\left(\sqrt{-\alpha\sigma}\Xi_j\right)^2\right\}e^{i\mathfrak{T}_j},$$

$$\Psi_2^{16}(x,t) = \pm 6\Pi\alpha\sigma(\ln(\mathscr{A}))^2\sqrt{-\frac{10\kappa p_1}{Y_2\mathscr{H}_1}}\left\{1-\tanh_{\mathscr{A}}\left(\sqrt{-\alpha\sigma}\Xi_j\right)^2\right\}e^{i\mathfrak{T}_j},$$

$$\Psi_1^{17}(x,t) = \pm 6\alpha\sigma(\ln(\mathscr{A}))^2\sqrt{-\frac{10\kappa p_1}{Y_2\mathscr{H}_1}}\left\{1-\coth_{\mathscr{A}}\left(\sqrt{-\alpha\sigma}\Xi_j\right)^2\right\}e^{i\mathfrak{T}_j},$$

$$\Psi_2^{17}(x,t) = \pm 6\Pi\alpha\sigma(\ln(\mathscr{A}))^2\sqrt{-\frac{10\kappa p_1}{Y_2\mathscr{H}_1}}\left\{1-\coth_{\mathscr{A}}\left(\sqrt{-\alpha\sigma}\Xi_j\right)^2\right\}e^{i\mathfrak{T}_j},$$

$$\Psi_1^{18}(x,t) = \pm 6\alpha\sigma(\ln(\mathscr{A}))^2\sqrt{-\frac{10\kappa p_1}{Y_2\mathscr{H}_1}}\left\{1-\left[-\tanh_{\mathscr{A}}\left(2\sqrt{-\alpha\sigma}\Xi_j\right)\pm i\sqrt{\mathscr{M}\mathscr{N}}\,\mathrm{sech}_{\mathscr{A}}\left(2\sqrt{-\alpha\sigma}\Xi_j\right)\right]^2\right\}e^{i\mathfrak{T}_j},$$

$$\Psi_2^{18}(x,t) = \pm 6\Pi\alpha\sigma(\ln(\mathscr{A}))^2\sqrt{-\frac{10\kappa p_1}{Y_2\mathscr{H}_1}}\left\{1-\left[-\tanh_{\mathscr{A}}\left(2\sqrt{-\alpha\sigma}\Xi_j\right)\pm i\sqrt{\mathscr{M}\mathscr{N}}\,\mathrm{sech}_{\mathscr{A}}\left(2\sqrt{-\alpha\sigma}\Xi_j\right)\right]^2\right\}e^{i\mathfrak{T}_j},$$

$$\Psi_1^{19}(x,t) = \pm 6\alpha\sigma(\ln(\mathscr{A}))^2\sqrt{-\frac{10\kappa p_1}{Y_2\mathscr{H}_1}}\left\{1-\left[-\coth_{\mathscr{A}}\left(2\sqrt{-\alpha\sigma}\Xi_j\right)\pm\sqrt{\mathscr{M}\mathscr{N}}\,\mathrm{csch}_{\mathscr{A}}\left(2\sqrt{-\alpha\sigma}\Xi_j\right)\right]^2\right\}e^{i\mathfrak{T}_j},$$

$$\Psi_2^{19}(x,t) = \pm 6\Pi\alpha\sigma(\ln(\mathscr{A}))^2\sqrt{-\frac{10\kappa p_1}{Y_2\mathscr{H}_1}}\left\{1-\left[-\coth_{\mathscr{A}}\left(2\sqrt{-\alpha\sigma}\Xi_j\right)\pm\sqrt{\mathscr{M}\mathscr{N}}\,\mathrm{csch}_{\mathscr{A}}\left(2\sqrt{-\alpha\sigma}\Xi_j\right)\right]^2\right\}e^{i\mathfrak{T}_j},$$

$$\Psi_1^{20}(x,t) = \pm\frac{3}{2}\alpha\sigma(\ln(\mathscr{A}))^2\sqrt{-\frac{10\kappa p_1}{Y_2\mathscr{H}_1}}\left\{4-\left[\tanh_{\mathscr{A}}\left(\frac{\sqrt{-\alpha\sigma}}{2}\Xi_j\right)+\coth_{\mathscr{A}}\left(\frac{\sqrt{-\alpha\sigma}}{2}\Xi_j\right)\right]^2\right\}e^{i\mathfrak{T}_j},$$

$$\Psi_2^{20}(x,t) = \pm\frac{3\Pi}{2}\alpha\sigma(\ln(\mathscr{A}))^2\sqrt{-\frac{10\kappa p_1}{Y_2\mathscr{H}_1}}\left\{4-\left[\tanh_{\mathscr{A}}\left(\frac{\sqrt{-\alpha\sigma}}{2}\Xi_j\right)+\coth_{\mathscr{A}}\left(\frac{\sqrt{-\alpha\sigma}}{2}\Xi_j\right)\right]^2\right\}e^{i\mathfrak{T}_j}. \tag{45}$$

Case 5. When $\sigma = \alpha$ and $\lambda = 0$,

$$\Psi_1^{21}(x,t) = \pm 6\alpha^2(\ln(\mathscr{A}))^2\sqrt{-\frac{10\kappa p_1}{Y_2\mathscr{H}_1}}\left\{\tan_{\mathscr{A}}\left(\alpha\Xi_j\right)^2+1\right\}e^{i\mathfrak{T}_j}, \tag{46}$$

$$\Psi_2^{21}(x,t) = \pm 6\Pi\alpha^2(\ln(\mathscr{A}))^2\sqrt{-\frac{10\kappa p_1}{Y_2\mathscr{H}_1}}\left\{\tan_{\mathscr{A}}\left(\alpha\Xi_j\right)^2+1\right\}e^{i\mathfrak{T}_j}, \tag{47}$$

$$\Psi_1^{22}(x,t) = \pm 6\alpha^2(\ln(\mathscr{A}))^2\sqrt{-\frac{10\kappa p_1}{Y_2\mathscr{H}_1}}\left\{\cot_{\mathscr{A}}\left(\alpha\Xi_j\right)^2+1\right\}e^{i\mathfrak{T}_j}, \tag{48}$$

$$\Psi_2^{22}(x,t) = \pm 6\Pi\alpha^2(\ln(\mathscr{A}))^2\sqrt{-\frac{10\kappa p_1}{Y_2\mathscr{H}_1}}\left\{\cot_{\mathscr{A}}\left(\alpha\Xi_j\right)^2+1\right\}e^{i\mathfrak{T}_j}, \tag{49}$$

$$\Psi_1^{23}(x,t) = \pm 6\alpha^2(\ln(\mathscr{A}))^2\sqrt{-\frac{10\kappa p_1}{Y_2\mathscr{H}_1}}\left\{\left[\tan_{\mathscr{A}}\left(2\alpha\Xi_j\right)\pm\sqrt{\mathscr{M}\mathscr{N}}\,\sec_{\mathscr{A}}\left(2\alpha\Xi_j\right)\right]^2+1\right\}e^{i\mathfrak{T}_j}, \tag{50}$$

$$\Psi_2^{23}(x,t) = \pm 6\Pi\alpha^2(\ln(\mathscr{A}))^2\sqrt{-\frac{10\kappa p_1}{Y_2\mathscr{H}_1}}\left\{\left[\tan_{\mathscr{A}}\left(2\alpha\Xi_j\right)\pm\sqrt{\mathscr{M}\mathscr{N}}\,\sec_{\mathscr{A}}\left(2\alpha\Xi_j\right)\right]^2+1\right\}e^{i\mathfrak{T}_j}, \tag{51}$$

$$\Psi_1^{24}(x,t) = \pm 6\alpha^2(\ln(\mathscr{A}))^2\sqrt{-\frac{10\kappa p_1}{Y_2\mathscr{H}_1}}\left\{\left[-\cot_{\mathscr{A}}\left(2\alpha\Xi_j\right)\pm\sqrt{\mathscr{M}\mathscr{N}}\,\mathrm{csc}_{\mathscr{A}}\left(2\alpha\Xi_j\right)\right]^2+1\right\}e^{i\mathfrak{T}_j}, \tag{52}$$

$$\Psi_2^{24}(x,t) = \pm 6\Pi\alpha^2(\ln(\mathscr{A}))^2\sqrt{-\frac{10\kappa p_1}{Y_2\mathscr{H}_1}}\left\{\left[-\cot_{\mathscr{A}}\left(2\alpha\Xi_j\right)\pm\sqrt{\mathscr{M}\mathscr{N}}\,\mathrm{csc}_{\mathscr{A}}\left(2\alpha\Xi_j\right)\right]^2+1\right\}e^{i\mathfrak{T}_j}, \tag{53}$$

$$\Psi_1^{25}(x,t) = \pm\frac{3}{2}\alpha^2(\ln(\mathscr{A}))^2\sqrt{-\frac{10\kappa p_1}{Y_2\mathscr{H}_1}}\left\{\left[\tan_{\mathscr{A}}\left(\frac{\alpha}{2}\Xi_j\right)-\cot_{\mathscr{A}}\left(\frac{\alpha}{2}\Xi_j\right)\right]^2+4\right\}e^{i\mathfrak{T}_j}, \tag{54}$$

$$\Psi_2^{25}(x,t) = \pm\frac{3\Pi}{2}\alpha^2(\ln(\mathscr{A}))^2\sqrt{-\frac{10\kappa p_1}{Y_2\mathscr{H}_1}}\left\{\left[\tan_{\mathscr{A}}\left(\frac{\alpha}{2}\Xi_j\right)-\cot_{\mathscr{A}}\left(\frac{\alpha}{2}\Xi_j\right)\right]^2+4\right\}e^{i\mathfrak{T}_j}. \tag{55}$$

Case 6. When $\sigma = -\alpha$ and $\lambda = 0$,

$$\Psi_1^{26}(x,t) = \pm 6\alpha^2(\ln(\mathscr{A}))^2\sqrt{-\frac{10\kappa p_1}{Y_2\mathscr{H}_1}}\left\{\tanh_{\mathscr{A}}\left(\alpha\Xi_j\right)^2-1\right\}e^{i\mathfrak{T}_j},$$

$$\Psi_2^{26}(x,t) = \pm 6\Pi\alpha^2(\ln(\mathscr{A}))^2\sqrt{-\frac{10\kappa p_1}{Y_2\mathscr{H}_1}}\left\{\tanh_{\mathscr{A}}\left(\alpha\Xi_j\right)^2-1\right\}e^{i\mathfrak{T}_j},$$

$$\Psi_1^{27}(x,t) = \pm 6\alpha^2(\ln(\mathscr{A}))^2\sqrt{-\frac{10\kappa p_1}{Y_2\mathscr{H}_1}}\left\{\coth_{\mathscr{A}}\left(\alpha\Xi_j\right)^2-1\right\}e^{i\mathfrak{T}_j},$$

$$\Psi_2^{27}(x,t) = \pm 6\Pi\alpha^2(\ln(\mathscr{A}))^2\sqrt{-\frac{10\kappa p_1}{Y_2\mathscr{H}_1}}\left\{\coth_{\mathscr{A}}\left(\alpha\Xi_j\right)^2-1\right\}e^{i\mathfrak{T}_j},$$

$$\Psi_1^{28}(x,t) = \pm 6\alpha^2(\ln(\mathscr{A}))^2\sqrt{-\frac{10\kappa p_1}{Y_2\mathscr{H}_1}}\left\{\left[-\tanh_{\mathscr{A}}\left(2\alpha\Xi_j\right)\pm i\sqrt{\mathscr{M}\mathscr{N}}\,\mathrm{sech}_{\mathscr{A}}\left(2\alpha\Xi_j\right)\right]^2-1\right\}e^{i\mathfrak{T}_j},$$

$$\Psi_2^{28}(x,t) = \pm 6\Pi\alpha^2(\ln(\mathscr{A}))^2\sqrt{-\frac{10\kappa p_1}{Y_2\mathscr{H}_1}}\left\{\left[-\tanh_{\mathscr{A}}\left(2\alpha\Xi_j\right)\pm i\sqrt{\mathscr{M}\mathscr{N}}\,\mathrm{sech}_{\mathscr{A}}\left(2\alpha\Xi_j\right)\right]^2-1\right\}e^{i\mathfrak{T}_j},$$

$$\Psi_1^{29}(x,t) = \pm 6\alpha^2(\ln(\mathscr{A}))^2\sqrt{-\frac{10\kappa p_1}{Y_2\mathscr{H}_1}}\left\{\left[-\coth_{\mathscr{A}}\left(2\alpha\Xi_j\right)\pm\sqrt{\mathscr{M}\mathscr{N}}\,\mathrm{csch}_{\mathscr{A}}\left(2\alpha\Xi_j\right)\right]^2-1\right\}e^{i\mathfrak{T}_j},$$

$$\Psi_2^{29}(x,t) = \pm 6\Pi\alpha^2(\ln(\mathscr{A}))^2\sqrt{-\frac{10\kappa p_1}{Y_2\mathscr{H}_1}}\left\{\left[-\coth_{\mathscr{A}}\left(2\alpha\Xi_j\right)\pm\sqrt{\mathscr{M}\mathscr{N}}\,\mathrm{csch}_{\mathscr{A}}\left(2\alpha\Xi_j\right)\right]^2-1\right\}e^{i\mathfrak{T}_j},$$

$$\Psi_1^{30}(x,t) = \pm\frac{3}{2}\alpha^2(\ln(\mathscr{A}))^2\sqrt{-\frac{10\kappa p_1}{Y_2\mathscr{H}_1}}\left\{\left[\tanh_{\mathscr{A}}\left(\frac{\alpha}{2}\Xi_j\right)+\coth_{\mathscr{A}}\left(\frac{\alpha}{2}\Xi_j\right)\right]^2-4\right\}e^{i\mathfrak{T}_j},$$

$$\Psi_2^{30}(x,t) = \pm\frac{3\Pi}{2}\alpha^2(\ln(\mathscr{A}))^2\sqrt{-\frac{10\kappa p_1}{Y_2\mathscr{H}_1}}\left\{\left[\tanh_{\mathscr{A}}\left(\frac{\alpha}{2}\Xi_j\right)+\coth_{\mathscr{A}}\left(\frac{\alpha}{2}\Xi_j\right)\right]^2-4\right\}e^{i\mathfrak{T}_j}. \tag{56}$$

Case 7. When $\lambda^2 = 4\alpha\sigma$ and

Case 8. When $\lambda = \alpha = 0$,

$$\Psi_1^{31}(x,t) = \pm 6\sqrt{-\frac{10\kappa p_1}{Y_2\mathscr{H}_1}}\frac{1}{\Xi_j^2}e^{i\mathfrak{T}_j},$$
$$\Psi_2^{31}(x,t) = \pm 6\Pi\sqrt{-\frac{10\kappa p_1}{Y_2\mathscr{H}_1}}\frac{1}{\Xi_j^2}e^{i\mathfrak{T}_j}. \tag{57}$$

Case 9. When $\lambda \neq 0$ and $\alpha = 0$,

$$\Psi_1^{32}(x,t) = \mp 6\lambda^2(\ln(\mathscr{A}))^2\mathscr{M}\sqrt{-\frac{10\kappa p_1}{Y_2\mathscr{H}_1}}\left\{\frac{\cosh_{\mathscr{A}}\left(\lambda\Xi_j\right)-\sinh_{\mathscr{A}}\left(\lambda\Xi_j\right)}{\left[\cosh_{\mathscr{A}}\left(\lambda\Xi_j\right)-\sinh_{\mathscr{A}}\left(\lambda\Xi_j\right)+\mathscr{M}\right]^2}\right\}e^{i\mathfrak{T}_j},$$

$$\Psi_2^{32}(x,t) = \mp 6\Pi\lambda^2(\ln(\mathscr{A}))^2\mathscr{M}\sqrt{-\frac{10\kappa p_1}{Y_2\mathscr{H}_1}}\left\{\frac{\cosh_{\mathscr{A}}\left(\lambda\Xi_j\right)-\sinh_{\mathscr{A}}\left(\lambda\Xi_j\right)}{\left[\cosh_{\mathscr{A}}\left(\lambda\Xi_j\right)-\sinh_{\mathscr{A}}\left(\lambda\Xi_j\right)+\mathscr{M}\right]^2}\right\}e^{i\mathfrak{T}_j},$$

$$\Psi_1^{33}(x,t) = \mp 6\lambda^2(\ln(\mathscr{A}))^2\mathscr{N}\sqrt{-\frac{10\kappa p_1}{Y_2\mathscr{H}_1}}\left\{\frac{\sinh_{\mathscr{A}}\left(\lambda\Xi_j\right)+\cosh_{\mathscr{A}}\left(\lambda\Xi_j\right)}{\left[\sinh_{\mathscr{A}}\left(\lambda\Xi_j\right)+\cosh_{\mathscr{A}}\left(\lambda\Xi_j\right)+\mathscr{N}\right]^2}\right\}e^{i\mathfrak{T}_j},$$

$$\Psi_2^{33}(x,t) = \mp 6\Pi\lambda^2(\ln(\mathscr{A}))^2\mathscr{N}\sqrt{-\frac{10\kappa p_1}{Y_2\mathscr{H}_1}}\left\{\frac{\sinh_{\mathscr{A}}\left(\lambda\Xi_j\right)+\cosh_{\mathscr{A}}\left(\lambda\Xi_j\right)}{\left[\sinh_{\mathscr{A}}\left(\lambda\Xi_j\right)+\cosh_{\mathscr{A}}\left(\lambda\Xi_j\right)+\mathscr{N}\right]^2}\right\}e^{i\mathfrak{T}_j}. \tag{58}$$

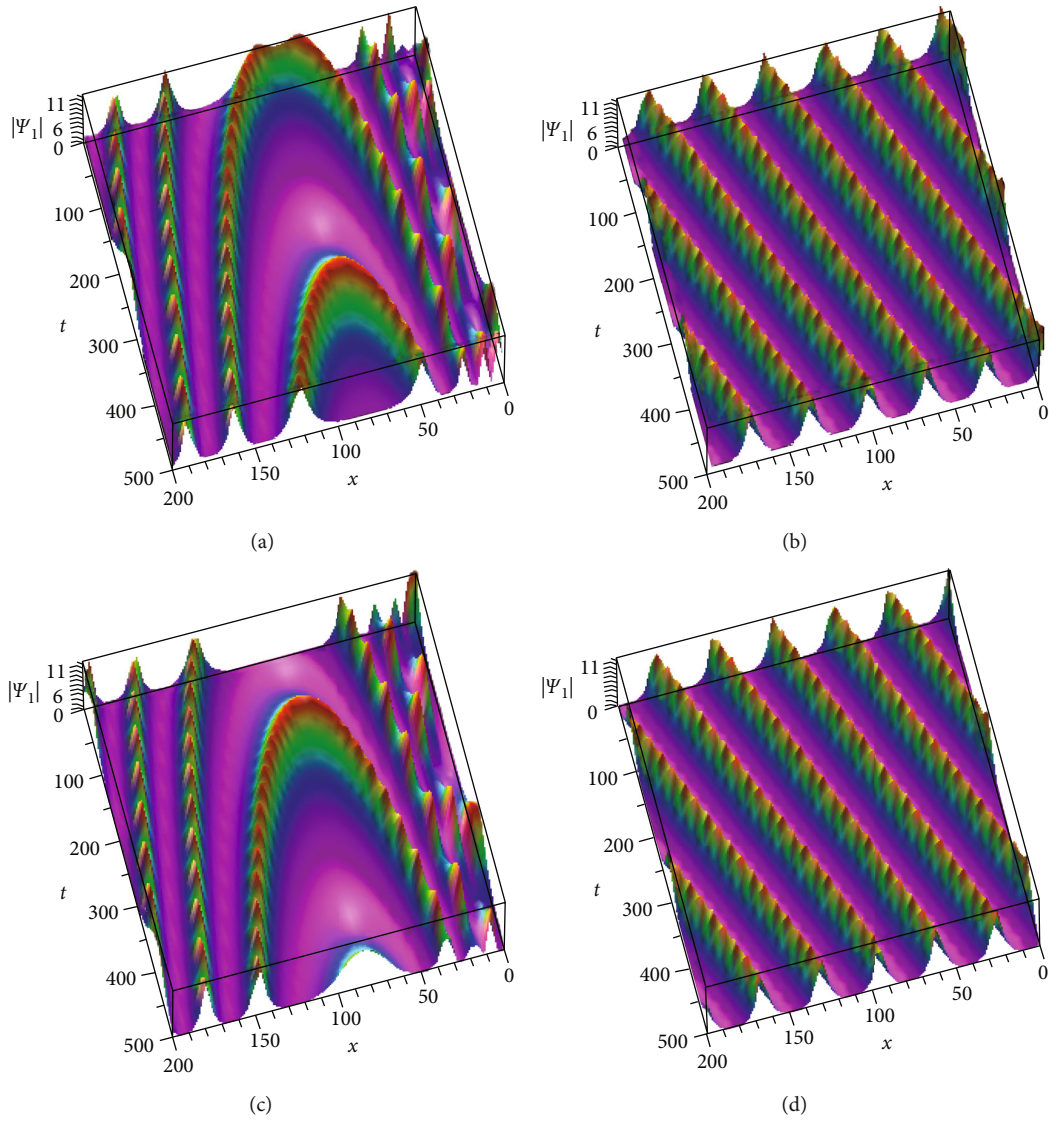

FIGURE 1: 3D periodic wave profile $|\Psi_1(x,t)|$ of Equation (26) for BFD parameter (a) $\mu = 0.9$, (b) $\mu = 1$ and CFD parameter (c) $\mu = 0.9$ and (d) $\mu = 1$ with other physical parameters by considering $\alpha = 2$, $\lambda = 1$, $\sigma = 3$, $\mathscr{A} = e$, $\mathscr{M} = 0.2$, $\mathscr{N} = 0.1$, $\kappa = 0.1$, $\Pi = 2$, $p_1 = r_1 = 0.2$, $s_1 = -0.3$, and $\theta_0 = 1$.

Case 10. When $\lambda = \mathscr{K}, \sigma = m\mathscr{K}(m \neq 0)$ and $\alpha = 0$,

$$\Psi_1^{34}(x,t) = \pm 6\mathscr{K}^2 m\mathscr{M}(\ln(\mathscr{A}))^2\sqrt{-\frac{10\kappa p_1}{Y_2\mathscr{K}_1}}\left\{\frac{m\mathscr{M}\mathscr{A}^{2\mathscr{K}\Xi_j}}{\left(\mathscr{M} - m\mathscr{N}\mathscr{A}^{\mathscr{K}\Xi_j}\right)^2} + \frac{\mathscr{A}^{\mathscr{K}\Xi_j}}{\mathscr{M} - m\mathscr{N}\mathscr{A}^{\mathscr{K}\Xi_j}}\right\}e^{i\mathfrak{T}_j},$$

$$\Psi_2^{34}(x,t) = \pm 6\Pi\mathscr{K}^2 m\mathscr{M}(\ln(\mathscr{A}))^2\sqrt{-\frac{10\kappa p_1}{Y_2\mathscr{K}_1}}\left\{\frac{m\mathscr{M}\mathscr{A}^{2\mathscr{K}\Xi_j}}{\left(\mathscr{M} - m\mathscr{N}\mathscr{A}^{\mathscr{K}\Xi_j}\right)^2} + \frac{\mathscr{A}^{\mathscr{K}\Xi_j}}{\mathscr{M} - m\mathscr{N}\mathscr{A}^{\mathscr{K}\Xi_j}}\right\}e^{i\mathfrak{T}_j}. \tag{59}$$

It is noted that all the obtained solutions are valid whenever $\kappa p_1 Y_2 \mathscr{K}_1 < 0$. Here, the formula for hyperbolic and trigonometric functions are defined as

$$\sinh_{\mathscr{A}}(\Xi) = \frac{\mathscr{M}\mathscr{A}^{\Xi} - \mathscr{N}\mathscr{A}^{-\Xi}}{2}, \cosh_{\mathscr{A}}(\Xi) = \frac{\mathscr{M}\mathscr{A}^{\Xi} + \mathscr{N}\mathscr{A}^{-\Xi}}{2},$$

$$\tanh_{\mathscr{A}}(\Xi) = \frac{\mathscr{M}\mathscr{A}^{\Xi} - \mathscr{N}\mathscr{A}^{-\Xi}}{\mathscr{M}\mathscr{A}^{\Xi} + \mathscr{N}\mathscr{A}^{-\Xi}}, \coth_{\mathscr{A}}(\Xi) = \frac{\mathscr{M}\mathscr{A}^{\Xi} + \mathscr{N}\mathscr{A}^{-\Xi}}{\mathscr{M}\mathscr{A}^{\Xi} - \mathscr{N}\mathscr{A}^{-\Xi}},$$

$$\sec h_{\mathscr{A}}(\Xi) = \frac{2}{\mathscr{M}\mathscr{A}^{\Xi} + \mathscr{N}\mathscr{A}^{-\Xi}}, \operatorname{csc} h_{\mathscr{A}}(\Xi) = \frac{2}{\mathscr{M}\mathscr{A}^{\Xi} - \mathscr{N}\mathscr{A}^{-\Xi}},$$

$$\sin_{\mathscr{A}}(\Xi) = \frac{\mathscr{M}\mathscr{A}^{i\Xi} - \mathscr{N}\mathscr{A}^{-i\Xi}}{2i}, \cos_{\mathscr{A}}(\Xi) = \frac{\mathscr{M}\mathscr{A}^{i\Xi} + \mathscr{N}\mathscr{A}^{-i\Xi}}{2},$$

$$\tan_{\mathscr{A}}(\Xi) = -i\frac{\mathscr{M}\mathscr{A}^{i\Xi} - \mathscr{N}\mathscr{A}^{-i\Xi}}{\mathscr{M}\mathscr{A}^{i\Xi} + \mathscr{N}\mathscr{A}^{-i\Xi}}, \cot_{\mathscr{A}}(\Xi) = i\frac{\mathscr{M}\mathscr{A}^{i\Xi} + \mathscr{N}\mathscr{A}^{-i\Xi}}{\mathscr{M}\mathscr{A}^{i\Xi} - \mathscr{N}\mathscr{A}^{-i\Xi}},$$

$$\sec_{\mathscr{A}}(\Xi) = \frac{2}{\mathscr{M}\mathscr{A}^{i\Xi} + \mathscr{N}\mathscr{A}^{-i\Xi}}, \operatorname{csc}_{\mathscr{A}}(\Xi) = \frac{2i}{\mathscr{M}\mathscr{A}^{i\Xi} - \mathscr{N}\mathscr{A}^{-i\Xi}}. \tag{60}$$

where Ξ is the independent variable and $\mathscr{M}, \mathscr{N} > 0$ are arbitrary constants called as deformation parameters.

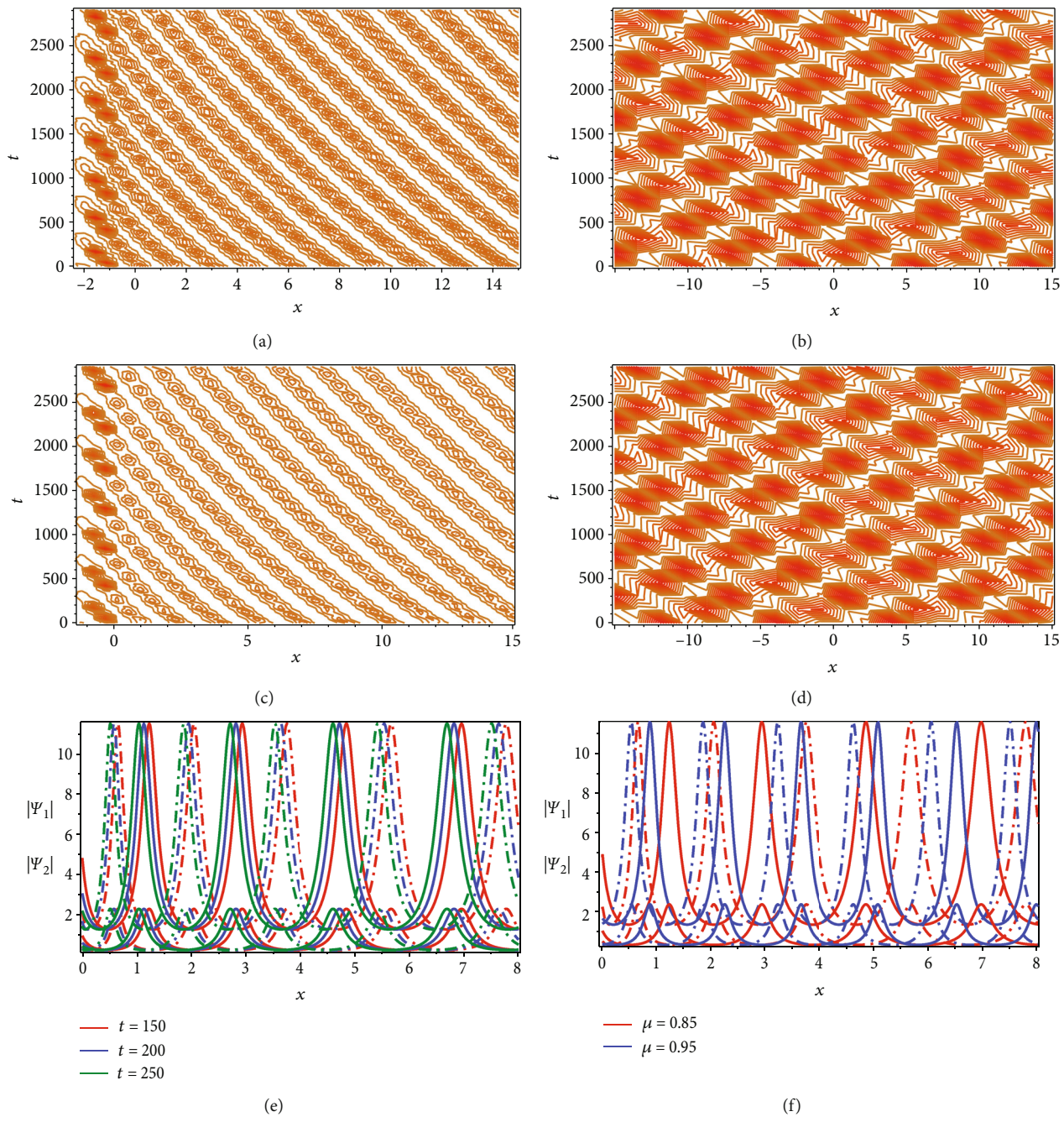

FIGURE 2: Contour plots of $|\Psi_1(x,t)|$ of Equation (26) for (a) $\mu = 0.9$ and (b) $\mu = 1$ for BFD, (c) $\mu = 0.9$ and (d) $\mu = 1$ for CFD, and 2D wave profile (Solid line = BFD; Dash Line = CFD) of the effect of (e) time for $\mu = 0.75$ and (f) fractional parameter μ for $t = 150$. The remaining parameters are as in Figure 1.

5. Graphical Representations and Discussions

Based on the attained hung amount of solitary wave solutions for the considered STF-CQNLSE in birefringent fibres with the sense of BFD and CFD, some of them are illustrated graphically (see Figures 1–6) for demonstrating the effectiveness of fractional parameter μ along with relevant physical discussions. In our analysis, the parametric values of μ are assumed as $0 < \mu \leq 1$ and the other free parameters are considered based on the conditions of EDAM.

Figures 1(a)–1(d) display the 3D periodic wave profiles $|\Psi_1(x,t)|$ by considering Equation (26) along with the influence of BFD parameter (CFD parameter) and $\alpha = 2$, $\lambda = 1$, $\sigma = 3$, $\mathscr{A} = e$, $\mathscr{M} = 0.2$, $\mathscr{N} = 0.1$, $\kappa = 0.1$, $\Pi = 2$, $p_1 = r_1 = 0.2$, $s_1 = -0.3$, $\theta_0 = 1$. In order to properly understand the influences of both BFD and CFD parameters, Figure 2 displays the contour plots and 2D wave profiles $|\Psi_1(x,t)|$ by considering the same Equation (26) and the same typical values of other parameter as in Figure 1. It is depicted from Figures 1 and 2 that the wavelength

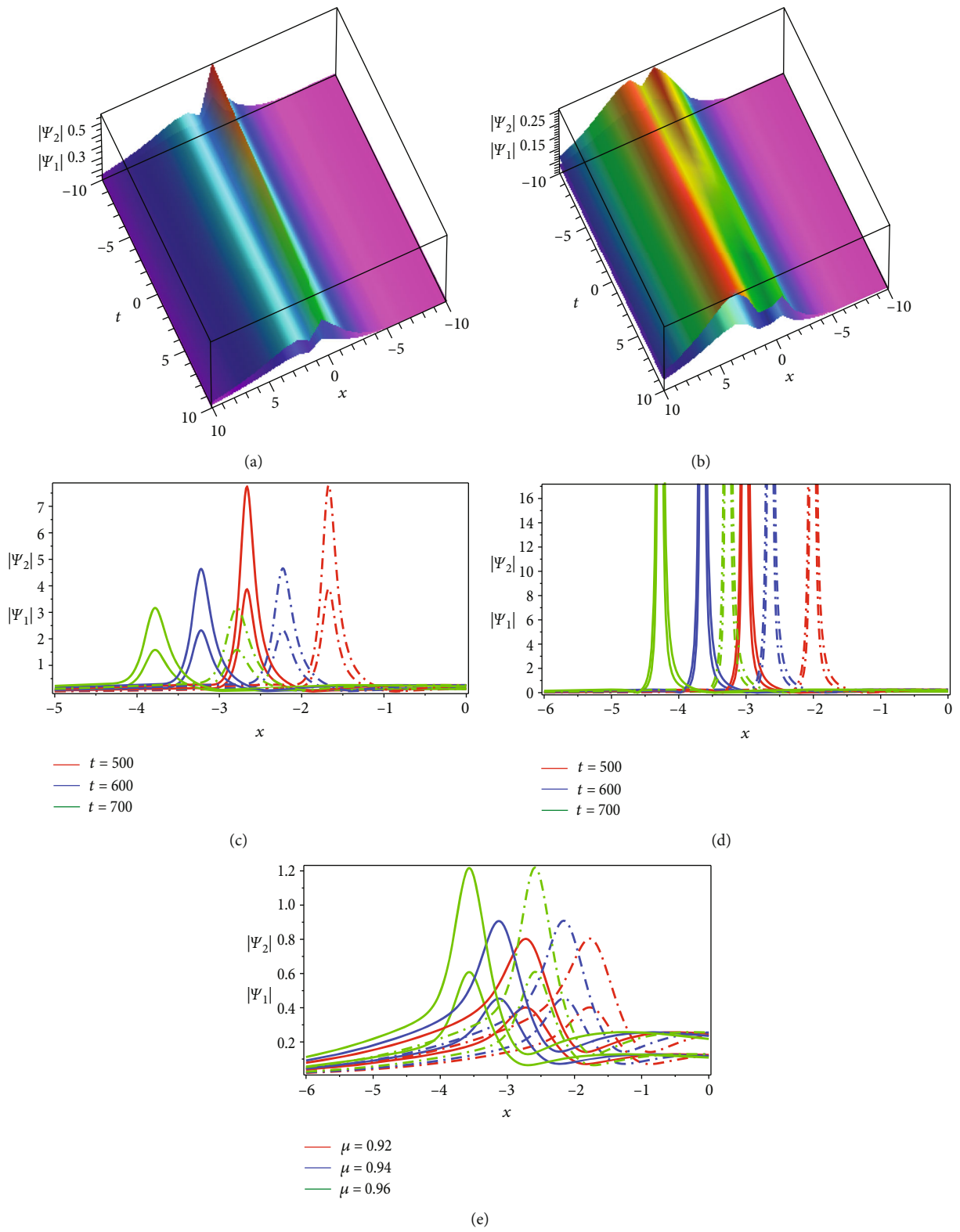

FIGURE 3: Optical rouge wave profiles of $|\Psi_1(x,t)|$ and $|\Psi_2(x,t)|$ as in Equation (38) and Equation (39), respectively, for (a) BFD parameter $\mu = 0.85$, (b) CFD parameter $\mu = 0.85$, the effect (solid line = BFD; dash line = CFD) of time for (c) $\mu = 0.98$ and (d) $\mu = 1$, (e) the effect of fractional parameter for $t = 750$. The remaining parameters are $\alpha = 0.1$, $\lambda = 0.5$, $\sigma = 0.2$, $\mathscr{A} = e$, $\mathscr{M} = -0.1$, $\mathscr{N} = 0.5$, $\kappa = 0.1$, $\Pi = 2$, $p_1 = 0.2$, $r_1 = -0.2$, $s_1 = 0.3$, and $\theta_0 = 1$.

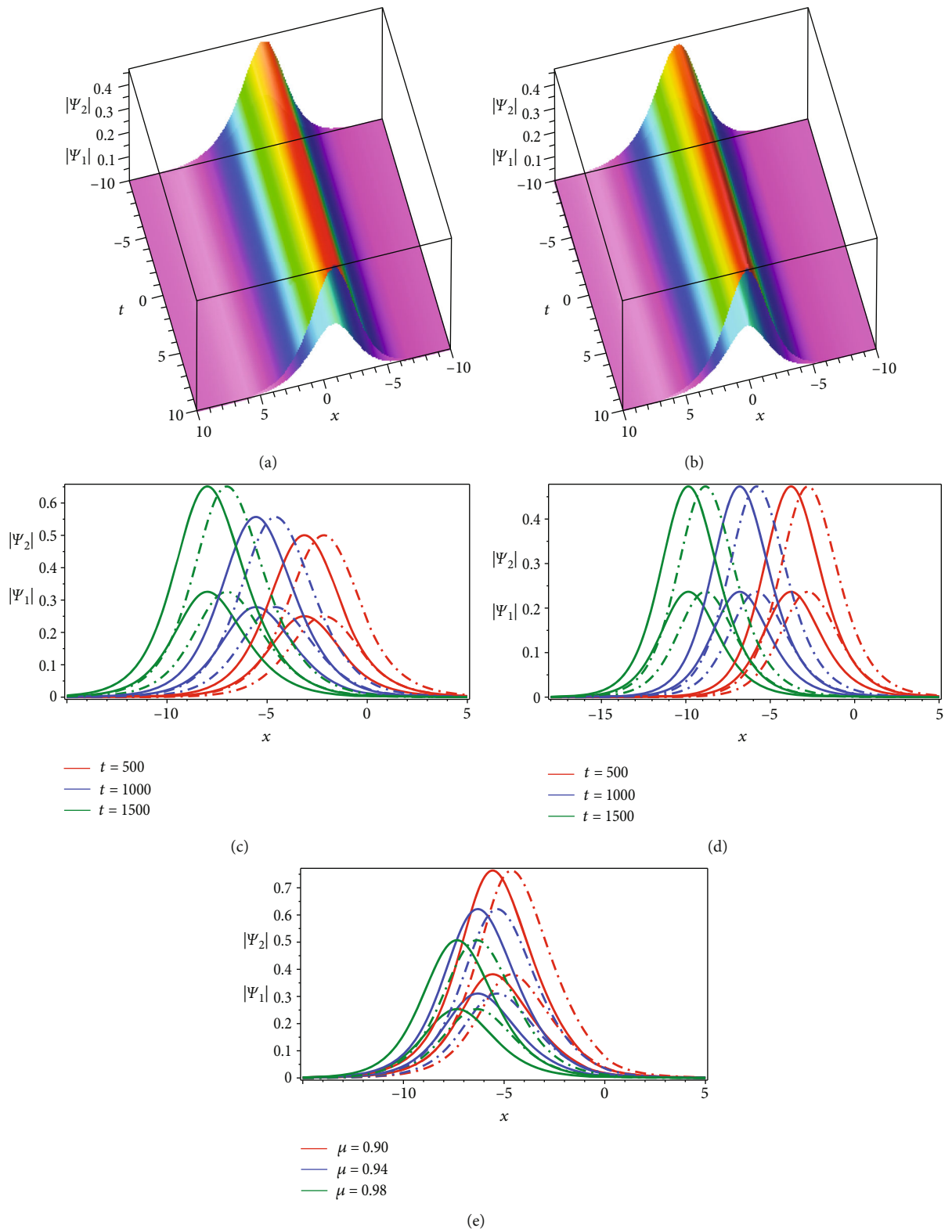

FIGURE 4: Optical bright soliton profiles of $|\Psi_1(x,t)|$ and $|\Psi_2(x,t)|$ as in Equation (40) and Equation (41), respectively, for (a) BFD parameter $\mu = 0.95$, (b) CFD parameter $\mu = 0.95$, the effect (Solid line = BFD; Dash Line = CFD) of time for (c) $\mu = 0.95$ and (d) $\mu = 1$, (e) the effect of fractional parameter for $t = 1200$. The remaining parameters are $\alpha = 0.1$, $\lambda = 0.9$, $\sigma = 0.5$, $\mathscr{A} = e$, $\mathscr{M} = \mathscr{N} = 1$, $\kappa = 0.1$, $\Pi = 2$, $p_1 = 0.2$, $r_1 = -0.2$, $s_1 = 0.3$, and $\theta_0 = 1$.

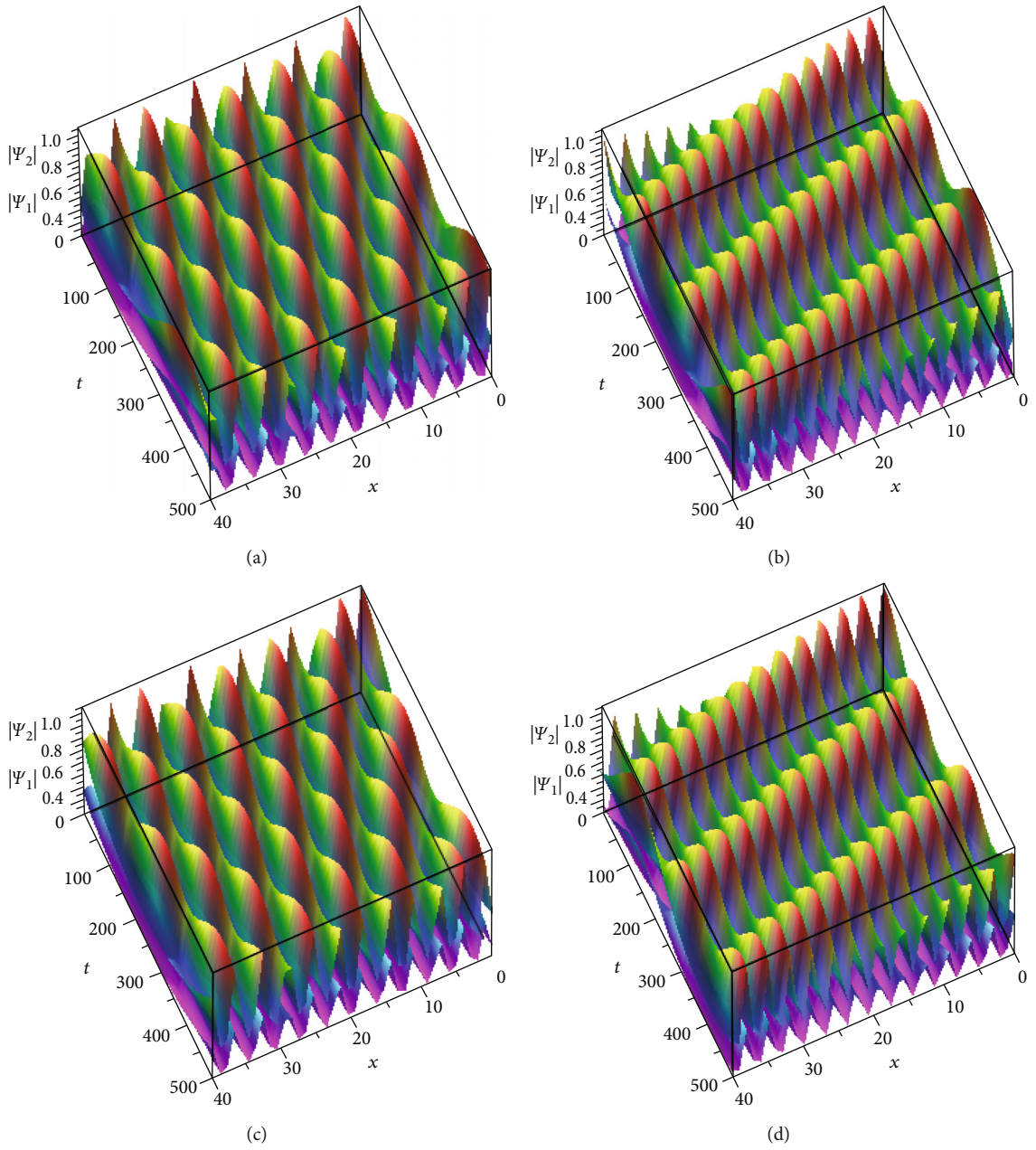

FIGURE 5: 3D periodic wave profiles of $|\Psi_1(x,t)|$ and $|\Psi_2(x,t)|$ as in Equation (54) and Equation (55), respectively, for BFD parameter (a) $\mu = 0.95$, (b) $\mu = 1$ and CFD parameter (c) $\mu = 0.95$, (d) $\mu = 1$. The other parameters are considered as $\alpha = \sigma = 0.5$, $\lambda = 0$, $\mathscr{A} = e$, $\mathscr{M} = 0.2$, $\mathscr{N} = 0.1$, $\kappa = 0.1$, $\Pi = 2$, $p_1 = r_1 = 0.2$, $s_1 = -0.3$, and $\theta_0 = 1$.

(frequency) are shorter (higher) for conformable derivative rather than beta derivative. In addition, the wavelength (frequency) are shorter (increasing) with the increase of both BFD and CFD parameter.

Figure 3 represents the 3D and 2D resonance solitary wave (like killer wave, singular soliton) profiles by considering Equation (38) and Equation (39) with the variation of both BFD and CFD parameter for time. To display these figures, the other parametric values are considered as $\alpha = 0.1$, $\lambda = 0.5$, $\sigma = 0.2$, $\mathscr{A} = e$, $\mathscr{M} = -0.1$, $\mathscr{N} = 0.5$, $\kappa = 0.1$, $\Pi = 2$, $p_1 = 0.2$, $r_1 = -0.2$, $s_1 = 0.3$, and $\theta_0 = 1$. It is interesting to show from Figure 3 that for different choice of arbitrary parameters, one can produce unstable soliton, that is, rouge waves for fractional value of the parameter μ from Equation (38) and Equation (39), but it would always produce singular soliton for $\mu = 1$. The amplitudes of rouge waves are increasing with regard to increase of fractional parameter, but decreasing and behaves pulse like with the increasing values of time.

Figure 4 presents the 3D and 2D resonance bright soliton profiles with the variation of time for both of BFD and CFD parameter by considering Equation (40) and Equation (41). To display these figures, the other parametric values are considered as $\alpha = 0.1$, $\lambda = 0.9$, $\sigma = 0.5$, $\mathscr{A} = e$, $\mathscr{M} = \mathscr{N} = 1$,

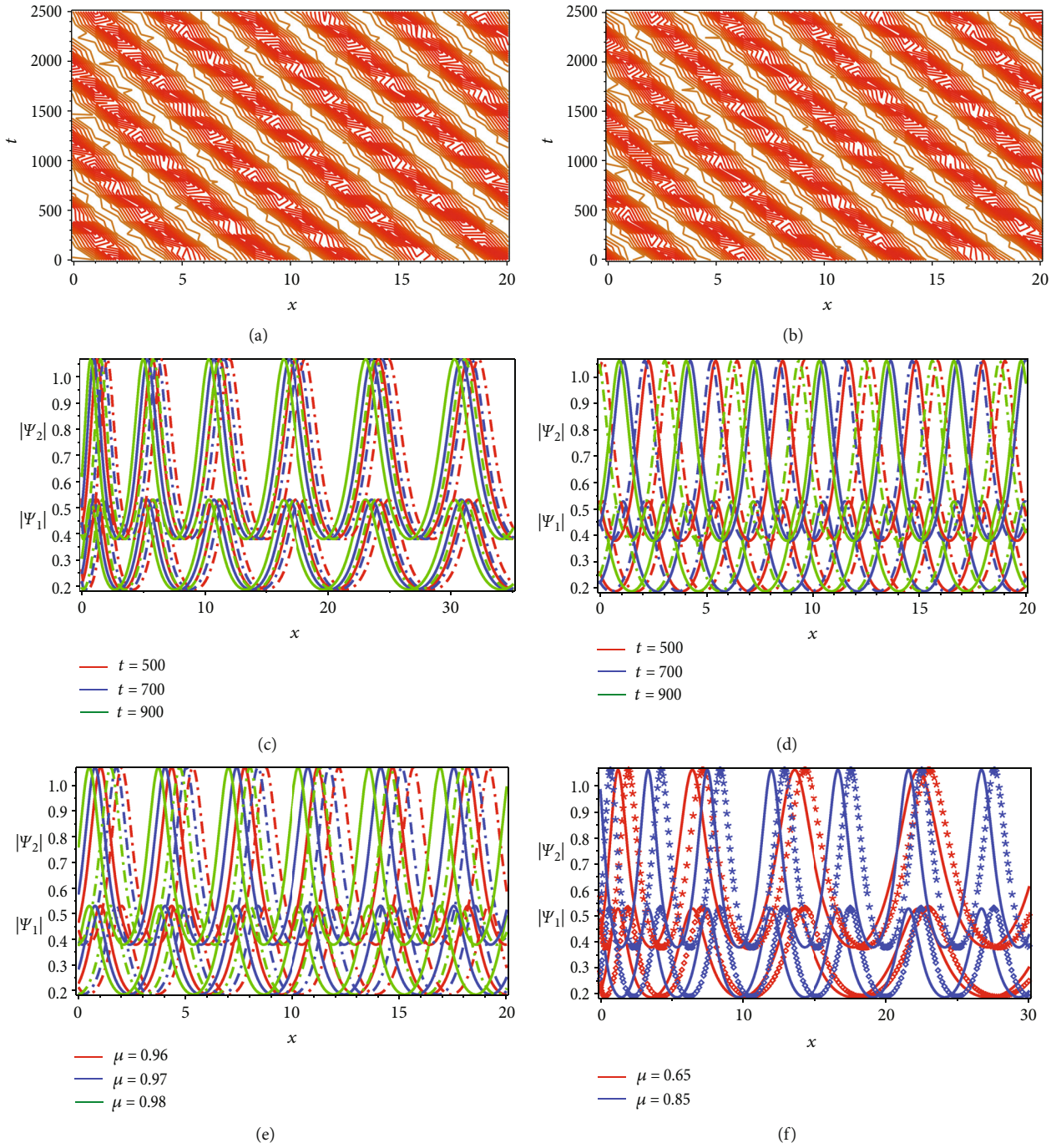

FIGURE 6: Contour plots of $|\Psi_1(x,t)|$ of Equation (54) for (a) BFD parameter $\mu = 0.95$ and (b) CFD parameter $\mu = 0.95$, and 2D wave profiles (solid line = BFD; dash line = CFD) with the effect of time for (c) $\mu = 0.75$, (d) $\mu = 1$ and (e, f) with the effect of fractional parameter for $t = 900$. The remaining parameters are as in Figure 5.

$\kappa = 0.1$, $\Pi = 2$, $p_1 = 0.2$, $r_1 = -0.2$, $s_1 = 0.3$, and $\theta_0 = 1$. It is depicted from Figure 4 that the amplitudes of bright solitons are decreasing with the increasing values of fractional parameter μ for any given time. For non-local value $\mu = 0.95$ of BFD (solid line) and CFD (dash line) parameter, the amplitudes of the bright solitons are increasing with pulse like behavior due to the increase of time. But, the amplitudes of the bright solitons are remaining constant and the bright solitons behaves pulse with the variation of time only for the local value of $\mu = 1$.

Finally, Figures 5 and 6 demonstrate the 3D contour plot and 2D resonance periodic wave profiles by considering Equation (54) and Equation (55) with the variation of both BFD and CFD parameter as well as time. To display these figures, the other parametric values are considered as $\alpha = \sigma = 0.5$, $\lambda = 0$, $\mathscr{A} = e$, $\mathscr{M} = 0.2$, $\mathscr{N} = 0.1$, $\kappa = 0.1$, $\Pi = 2$,

$p_1 = r_1 = 0.2$, $s_1 = -0.3$, and $\theta_0 = 1$. It is depicted from Figures 5 and 6 that soliton types periodic waves are produced for any values of BFD and CFD parameter and the increasing values of time. But, only the wavelength of such waves are increasing along the space domain for a specific time with a fractional value of the BFD and CFD parameter. Further, the wavelength of these waves are remarkably decreased when the values of the fractional parameter are sufficiently increased. It is also observed that the frequency of these waves are increased dramatically for local value $\mu = 1$ rather than any nonlocal value of BFD and CFD parameter. Consequently, Figure 6(f) is clearly shown that the blue light (short wavelength) travels faster than red light (long wavelength).

It is noted that Yildirim et al. [23] have only secured dark and singular type optical solitons by adopting exp-function expansion algorithm. In another report [24], they recovered bright, dark, and singular solitons by Riccati function approach, sine-Gordon function technique, and F-expansion scheme. Additionally, Zahran and Bekir [25] implemented extended simple equation method to recover some periodic and singular type solutions by taking four forms of nonlinearity. But in all these studies, their model equation is identical with this considered STF-CQNLSE when the parametric value $\mu = 1$ is taken only. Further, Dutta et al. [26] have also investigated similar types of solutions by considering the equation for parabolic law nonlinearity having conformable derivative by utilizing the extended sinh-Gordon expansion method. But the novelty of the current study is that we investigate more new solitonic structures, like periodic pulse, combo bright-dark, rogue structures, etc. along with their obtained solutions based on the existence criteria of the solutions as well as some parametric values which were not found in previous literatures. We also illustrated whether there is any effect of the fractional parameter in the equation considered and found that it has a considerable impact on the optical wave structures. This new EDAM technique is being implemented for the first time to derive several forms of optical solitons from the considered model equation, and some of the solutions return similar wave structures for other techniques suggested in the literature. Thus, the derived solutions take on an entirely new form because of the fractional order. As a result, this technique can be utilized to construct more general forms of solutions not only for the STF-CQNLSE under consideration, but also for any model equation in other disciplines.

6. Concluding Remarks

The classical derivative operators are sometimes unable to address the physical issues in the dynamical systems. This actually happens when the complexity may arise suddenly in a certain regime of space or time due to the impact of nonlocality or nonconservative energies or any other physical reasons in birefringent fibres. To overcome such difficulty, one may use the fractal, or so-called the BFD and CFD. Such derivatives are treated as the local or nonlocal derivatives based on the parametric value of fractional parameter. Thus, the coupled cubic-quartic nonlinear Schrödinger equations having Kerr-law nonlinearity and both of BFD and CFD space–time evolution have been considered to study the optical pulses in birefringent fibers. The effective integration scheme, that is EDAM has been successfully implemented to determine the optical wave solutions. It is observed that the fractal nonlocal operator parameter is remarkably changed the optical wave phenomena in birefringent fibres. In this way, one may study optical wave phenomena in birefringent fibres by considering the presented model having other nonlinearities. Note that some useful new solutions have been determined by considering the constraint conditions. However, one can study the stability analysis for traveling waves by forming the planar dynamical system, but beyond the scope of this study.

Data Availability

No new data were created or analyzed in this study.

Conflicts of Interest

The authors declare that there is no conflict of interest.

References

[1] A. Biswas and S. Konar, *Introduction to Non-Kerr Law Optical Solitons*, Chapman and Hall/CRC Press, New York, 2006.

[2] G. P. Agrawal, *Nonlinear Fiber Optics*, Academic Press, New York, 2007.

[3] Q. Zhou, D. Yao, F. Chen, and W. Li, "Optical solitons in gas-filled, hollow-core photonic crystal fibers with inter-modal dispersion and self-steepening," *Journal of Modern Optics*, vol. 60, no. 10, pp. 854–859, 2013.

[4] M. F. Uddin, M. G. Hafez, Z. Hammouch, H. Rezazadeh, and D. Baleanu, "Traveling wave with beta derivative spatial-temporal evolution for describing the nonlinear directional couplers with metamaterials via two distinct methods," *Alexandria Engineering Journal*, vol. 60, no. 1, pp. 1055–1065, 2021.

[5] S. Ozgul, M. Turan, and A. Yildirim, "Exact traveling wave solutions of perturbed nonlinear Schrodinger's equation (NLSE) with Kerr law nonlinearity," *Optik*, vol. 123, no. 24, pp. 2250–2253, 2012.

[6] M. Eslami, "Solitary wave solutions for perturbed nonlinear Schrodinger's equation with Kerr law nonlinearity under the DAM," *Optik*, vol. 126, no. 13, pp. 1312–1317, 2015.

[7] A. Biswas, Q. Zhou, M. Z. Ullah, H. Triki, S. P. Moshokoa, and M. Belic, "Optical soliton perturbation with anti-cubic nonlinearity by semi-inverse variational principle," *Optik*, vol. 143, pp. 131–134, 2017.

[8] N. Raza and A. Javid, "Dynamics of optical solitons with Radhakrishnan-Kundu-Lakshmanan model via two reliable integration schemes," *Optik*, vol. 178, pp. 557–566, 2019.

[9] J. G. Liu, M. S. Osman, and A. M. Wazwaz, "A variety of non-autonomous complex wave solutions for the (2+1)-dimensional nonlinear Schrodinger equation with variable coefficients in nonlinear optical fibers," *Optik*, vol. 180, pp. 917–923, 2019.

[10] C. R. Menyuk, "Stability of solitons in birefringent optical fibers. I: equal propagation amplitudes," *Optics Letters*, vol. 12, no. 8, pp. 614–616, 1987.

[11] M. N. Islam, C. D. Poole, and J. P. Gordon, "Soliton trapping in birefringent optical fibers," *Optics Letters*, vol. 14, no. 18, pp. 1011–1013, 1989.

[12] Y. Barad and Y. Silberberg, "Polarization evolution and polarization instability of solitons in a birefringent optical fiber," *Physical Review Letters*, vol. 78, no. 17, pp. 3290–3293, 1997.

[13] Y. Jiang, B. Tian, W. J. Liu, K. Sun, and P. Wang, "Mixed-type solitons for the coupled higher–order nonlinear Schrödinger equations in multi-mode and birefringent fibers," *Journal of Modern Optics*, vol. 60, no. 8, pp. 629–636, 2013.

[14] M. S. Mani Rajan, J. Hakkim, A. Mahalingam, and A. Uthayakumar, "Dispersion management and cascade compression of femtosecond nonautonomous soliton in birefringent fiber," *The European Physical Journal D*, vol. 67, no. 7, p. 150, 2013.

[15] A. Biswas, K. R. Khan, A. Rahman, A. Yildirim, T. Hayat, and O. M. Aldossary, "Bright and dark optical solitons in birefringent fibers with Hamiltonian perturbations and Kerr law nonlinearity," *Journal of Optoelectronics and Advanced Materials*, vol. 14, pp. 571–576, 2012.

[16] A. H. Bhrawy, A. A. Alshaery, E. M. Hilal et al., "Optical solitons in birefringent fibers with spatio-temporal dispersion," *Optik*, vol. 125, no. 17, pp. 4935–4944, 2014.

[17] A. Biswas, A. H. Kara, M. Z. Ullah, Q. Zhou, H. Triki, and M. Belic, "Conservation laws for cubic-quartic optical solitons in Kerr and power law media," *Optik*, vol. 145, pp. 650–654, 2017.

[18] A. Biswas, H. Triki, Q. Zhou, S. P. Moshokoa, M. Z. Ullah, and M. Belic, "Cubic-quartic optical solitons in Kerr and power law media," *Optik*, vol. 144, pp. 357–362, 2017.

[19] O. Gonzalez-Gaxiola, A. Biswas, F. Mallawi, and M. R. Belic, "Cubic-quartic bright optical solitons with improved Adomian decomposition method," *Journal of Advanced Research*, vol. 21, pp. 161–167, 2020.

[20] E. M. E. Zayed, R. M. A. Shohib, and M. E. M. Alngar, "Solitons in optical fiber Bragg gratings for perturbed NLSE having cubic- quartic dispersive reflectivity with parabolic-nonlocal combo law of refractive index," *Optik*, vol. 243, article 167406, 2021.

[21] E. M. E. Zayed, R. M. A. Shohib, M. E. M. Alngar, T. A. Nofal, and K. A. Gepreel, "Cubic-quartic optical solitons in magneto-optic waveguides for NLSE with Kudryashov's law arbitrary refractive index and generalized non-local laws of nonlinearity," *Optik*, vol. 261, article 169127, 2022.

[22] E. M. E. Zayed, R. M. A. Shohib, M. E. M. Alngar, T. A. Nofal, K. A. Gepreel, and Y. Yildirim, "Cubic-quartic optical solitons with Biswas-Milovic equation having dual-power law nonlinearity using two integration algorithms," *Optik*, vol. 265, article 169453, 2022.

[23] Y. Yildirim, A. Biswas, A. J. M. Jawad et al., "Cubic-quartic optical solitons in birefringent fibers with four forms of nonlinear refractive index by exp-function expansion," *Results in Physics*, vol. 16, article 102913, 2020.

[24] Y. Yildirim, A. Biswas, P. Guggilla, F. Mallawi, and M. R. Belic, "Cubic-quartic optical solitons in birefringent fibers with four forms of nonlinear refractive index," *Optik*, vol. 203, article 163885, 2020.

[25] E. H. M. Zahran and A. Bekir, "New private types for the cubic-quartic optical solitons in birefringent fibers in its four forms of nonlinear refractive index," *Optical and Quantum Electronics*, vol. 53, no. 12, p. 680, 2021.

[26] H. Dutta, H. Günerhan, K. K. Ali, and R. Yilmazer, "Exact soliton solutions to the cubic-quartic non-linear Schrödinger equation with conformable derivative," *Frontiers of Physics*, vol. 8, p. 62, 2020.

[27] E. M. E. Zayed, M. E. M. Alngar, R. M. A. Shohib et al., "Cubic-quartic optical solitons in birefringent fibers with Sasa-Satsuma equation," *Optik*, vol. 261, article 169230, 2022.

[28] I. Podlubny, *Fractional Differential Equations: An Introduction to Fractional Derivatives, Fractional Differential Equations, to Methods of their Solution and some of their Applications*, Academic Press, New York, 1998.

[29] K. B. Oldham and J. Spanier, *The Fractional Calculus*, Academic Press, New York, 1974.

[30] M. Caputo and F. Mainardi, "A new dissipation model based on memory mechanism," *Pure and Applied Geophysics*, vol. 91, no. 1, pp. 134–147, 1971.

[31] E. Bas, B. Acay, and R. Ozarslan, "Fractional models with singular and nonsingular kernels for energy efficient buildings," *Chaos*, vol. 29, no. 2, article 023110, 2019.

[32] A. Atangana and D. Baleanu, "New fractional derivatives with nonlocal and nonsingular kernel," *Theory and Application to Heat Transfer Model Thermal Science*, vol. 20, pp. 763–769, 2016.

[33] M. F. Uddin, M. G. Hafez, I. Hwang, and C. Park, "Effect of space fractional parameter on nonlinear ion acoustic shock wave excitation in an unmagnetized relativistic plasma," *Frontiers of Physics*, vol. 9, article 766035, 2022.

[34] M. F. Uddin, M. G. Hafez, and S. A. Iqbal, "Dynamical plane wave solutions for the Heisenberg model of ferromagnetic spin chains with beta derivative evolution and obliqueness," *Heliyon*, vol. 8, no. 3, article e09199, 2022.

[35] M. F. Uddin, M. G. Hafez, Z. Hammouch, and D. Baleanu, "Periodic and rogue waves for Heisenberg models of ferromagnetic spin chains with fractional beta derivative evolution and obliqueness," *Waves in Random and Complex Media*, vol. 31, no. 6, pp. 2135–2149, 2021.

[36] M. F. Uddin and M. G. Hafez, "Interaction of complex short wave envelope and real long wave described by the coupled Schrodinger-Boussinesq equation with variable coefficients and beta space fractional evolution," *Results in Physics*, vol. 19, article 103268, 2020.

[37] M. G. Hafez, S. A. Iqbal, S. Akther, and M. F. Uddin, "Oblique plane waves with bifurcation behaviors and chaotic motion for resonant nonlinear Schrodinger equations having fractional temporal evolution," *Results in Physics*, vol. 15, article 102778, 2019.

[38] S. A. Iqbal, M. G. Hafez, and M. F. Uddin, "Bifurcation features, chaos, and coherent structures for one-dimensional nonlinear electrical transmission line," *Computational and Applied Mathematics*, vol. 41, no. 1, p. 50, 2022.

[39] H. Rezazadeh, "New solitons solutions of the complex Ginzburg-Landau equation with Kerr law nonlinearity," *Optik*, vol. 167, pp. 218–227, 2018.

[40] W.-B. Bo, R.-R. Wang, Y. Fang, Y. Y. Wang, and C. Q. Dai, "Prediction and dynamical evolution of multipole soliton families in fractional Schrödinger equation with the PT-symmetric

potential and saturable nonlinearity," *Nonlinear Dynamics*, 2022.

[41] W.-B. Bo, W. Liu, and Y.-Y. Wang, "Symmetric and antisymmetric solitons in the fractional nonlinear Schrodinger equation with saturable nonlinearity and PT-symmetric potential: stability and dynamics," *Optik*, vol. 255, article 168697, 2022.

[42] B.-H. Wang and Y.-Y. Wang, "Fractional white noise functional soliton solutions of a wick-type stochastic fractional NLSE," *Applied Mathematics Letters*, vol. 110, article 106583, 2020.

[43] H. Yépez-Martínez, A. Pashrashid, J. F. Gómez-Aguilar, L. Akinyemi, and H. Rezazadeh, "The novel soliton solutions for the conformable perturbed nonlinear Schrödinger equation," *Modern Physics Letters B*, vol. 36, no. 8, article 2150597, 2022.

[44] A. Akbulut, S. M. R. Islam, H. Rezazadeh, and F. Taşcan, "Obtaining exact solutions of nonlinear partial differential equations via two different methods," *International Journal of Modern Physics B*, vol. 36, no. 5, article 2250041, 2022.

[45] A. Abdeljabbar, H. O. Roshid, and A. Aldurayhim, "Bright, dark, and rogue wave soliton solutions of the quadratic nonlinear Klein–Gordon equation," *Symmetry*, vol. 14, no. 6, p. 1223, 2022.

[46] Z. Rahman, M. Z. Ali, H.-O. Roshid, M. S. Ullah, and X.-Y. Wen, "Dynamical structures of interaction wave solutions for the two extended higher-order KdV equations," *Pramana*, vol. 95, no. 3, pp. 1–14, 2021.

[47] M. S. Ullah, M. Z. Ali, H. O. Roshid, and M. F. Hoque, "Collision phenomena among lump, periodic and stripe soliton solutions to a (2 + 1)-dimensional Benjamin–Bona–Mahony–burgers model," *The European Physical Journal Plus*, vol. 136, no. 4, p. 370, 2021.

[48] A. Atangana, D. Baleanu, and A. Alsaedi, "Analysis of time-fractional hunter-Saxton equation: a model of neumatic liquid crystal," *Open Physics*, vol. 14, no. 1, pp. 145–149, 2016.

[49] R. Khalil, M. Al-Horani, A. Yousef, and M. Sababheh, "A new definition of fractional derivative," *Journal of Computational and Applied Mathematics*, vol. 264, pp. 65–70, 2014.